NOVA SCHOOL OF SCIENCE & TECHNOLOGY

DEPARTMENT OF PHYSICS

MARIANA SANTOS MENDES

BSc in Biomedical Engineering

# LIGHT-RESPONSIVE ON-DEMAND DRUG-DELIVERY SYSTEMS FOR DERMAL APPLICATIONS

MASTER IN BIOMEDICAL ENGINEERING

NOVA University Lisbon
October, 2023

NOVA SCHOOL OF SCIENCE & TECHNOLOGY

DEPARTMENT OF PHYSICS

# LIGHT-RESPONSIVE ON-DEMAND DRUG-DELIVERY SYSTEMS FOR DERMAL APPLICATIONS

**MARIANA SANTOS MENDES**

BSc in Biomedical Engineering

**Adviser:** Ana Catarina Bernardino Baptista
*Researcher, NOVA University Lisbon*

**Co-adviser:** Isabel Ferreira
*Associate Professor, NOVA University Lisbon*

**Examination Committee**

**Chair:** Célia Maria Reis Henriques
*Associate Professor, NOVA University Lisbon*

**Rapporteur:** Ana Patrícia Correia Almeida
*Junior Researcher, NOVA University Lisbon*

**Member:** Ana Catarina Bernardino Baptista
*Researcher, NOVA University Lisbon*

MASTER IN BIOMEDICAL ENGINEERING

NOVA University Lisbon
October, 2023

**Light-responsive on-demand drug-delivery systems for dermal applications**



This document was created with the (pdf/Xe/Lua)LaTeX processor and the NOVAthesis template (v6.10.17) [1].

Para a minha família e amigos,

# Acknowledgements

Em primeiro lugar, quero agradecer à minha orientadora professora Ana Baptista e à minha coorientadora professora Isabel Ferreira pelo apoio e orientação que me deram na escrita desta tese, não podia ter escolhido melhores docentes para me guiar neste percurso.

Para a minha família, por me terem dado a possibilidade de embarcar nesta viagem que agora chega ao fim. Pais, mana, avó, devo-vos tudo, obrigada!

Ao Dnis, sofreste tanto ao ter que aturar a rapariga mais miserável à face da Terra (principalmente durante a escrita)! Obrigada por todo o apoio, conselhos (mesmo que achas que não os ouvia e aplicava), motivação e conforto que me deste, e espero que continues a dar, durante estes anos, teria sido mesmo miserável se não estivesses lá para mim.

Ao Broken Cross, companheiros desta grande viagem, parece que estou a escrever fitas outra vez, as lágrimas vêm aos olhos por esta Era estar mesmo a chegar ao fim. Obrigada por fazerem parte da minha casa fora de casa. Louis, Gouveia e Martinha, todo o sofrimento valeu a pena porque vos conheci, ao melhor colega de grupo e dançarino, à melhor colega de casa e cantora, à pessoa mais fofa que conheço, um obrigada do fundo do coração por estes 5 anos magníficos mas não ficamos por aqui.

Ao Marlau Catmar, apesar de estarem longe e não terem acompanhado este 5 anos de perto sinto que tenho na mesma de vos agradecer por todos os anos de amizade, pelos verões bem passados que me carregavam as energias para mais um ano de faculdade e por alegrarem os meus dias com os mexericos no grupo.

Este trabalho foi realizado no âmbito do projeto "All-Fiber Integrated Photovoltaic Storage Devices for e-Textiles" de referência PTDC/CTM-CTM/157/2020, financiado por fundos nacionais via FCT, IP.

# Abstract

Chronic wounds are portrayed as an anomaly in the healing process. Economically speaking this type of wounds lead to a burden in the healthcare system due to the need of specialised clinicians and the overall cost of the treatment. Furthermore, the patient undergoes notable physical and emotional discomfort.

The employment of Drug Delivery Systems (DDSs) in patch form can be advantageous in this condition as it can provide a boundary between the environment and the body, maintaining the correct moisture, and supplying the necessary drugs with a lower periodicity. The use of light as the stimuli to release the therapeutic agent brings an added value to the DDSs as it has a noninvasive nature, it's efficiently applied and has a high spacial and temporal control.

With the above information in mind, the present work consisted in the development, through the electrospinning and electrospray techniques, and characterization of Cellulose Acetate (CA)+Ibuprofen (Ibu)+Poly(3-hexylthiophene) (P3HT) membranes for controlled drug release.

Regarding the drug release tests, with the use of Ultraviolet (UV) light a increase in the Ibu concentration was observed in all the membranes when compared with the respective passive release values. In the infrared light test, CA+Ibu+P3HT(spray) and CA+Ibu+P3HT(blend) membranes don't reach their passive values, while the CA+Ibu and CA membrane reach and surpasse the passive value, respectively.

This work presents good prospects for application in dermal treatment, but it is necessary to carry out additional studies, such as cytotoxicity analysis and optimization of the morphological and electrical properties of the membranes produced.

**Keywords:** Controlled drug release, electrospinning, cellulose acetate, ibuprofen, P3HT, light stimuli

# Resumo

As feridas crônicas são retratadas como uma anomalia no processo de cicatrização. Economicamente, este tipo de ferida leva a um fardo no sistema de saúde devido à necessidade de profissionais especializados e ao custo geral do tratamento. Além disso, o paciente enfrenta um significativo desconforto físico e emocional.

A utilização de sistemas de entrega de fármaco em forma de adesivo pode ser vantajosa neste caso, pois pode fornecer uma barreira entre o ambiente e o corpo, mantendo a humidade adequada e fornecendo o fármaco necessário com menor periodicidade. O uso da luz como estímulo para liberar o agente terapêutico traz um valor adicional aos sistemas de entrega de fármaco, pois possui uma natureza não invasiva, é aplicado de forma eficiente e possui alto controlo espacial e temporal.

Com as informações acima em mente, o presente trabalho consistiu no desenvolvimento, por meio das técnicas de *electrospinning* e *eletrospray*, e na caracterização de membranas de AC+Ibu+P3HT para libertação controlada de fármaco.

Em relação aos testes de libertação de fármaco, com o uso da luz UV, foi observado um aumento na concentração de Ibu em todas as membranas quando comparado aos respectivos valores de libertação passiva. No teste de luz infravermelha, as membranas de AC+Ibu+P3HT (spray) e AC+Ibu+P3HT (mistura) não atingem os seus valores passivos, enquanto as membranas de AC+Ibu e AC alcançam e superam o valor passivo, respectivamente.

Este trabalho apresenta boas perspectivas para aplicação no tratamento dermatológico, mas é necessário realizar estudos adicionais, como análise de citotoxicidade e otimização das propriedades morfológicas e elétricas das membranas produzidas.

**Palavras-chave:** Libertação controlada de fármaco, electrofiação, acetato de celulose, ibuprofeno, P3HT, estímulo luminoso

# Contents

# List of Figures

# List of Tables

# Abbreviations

**Au** Gold *(p. 10)*

**CA** Cellulose Acetate *(pp. v, ix, xi, 4, 5, 7, 8, 10, 11, 15–20, 22, 26–30, 35)*

**DCM** Dichloromethane *(pp. 8, 19)*
**DDSs** Drug Delivery Systems *(pp. v, 1–5, 7)*
**DMAc** Dimethylacetamide *(pp. 7, 8)*

**I-V Curve** Current-Voltage Characteristic Curve *(pp. 7, 11)*
**Ibu** Ibuprofen *(pp. v, vi, ix, 4–8, 11, 13, 15–20, 22–25, 27–30, 35)*

**MFD** Mean Fiber Diameter *(pp. 16–19, 30)*

**NIR** Near-Infrared *(pp. 2–4, 11, 35)*

**P3HT** Poly(3-hexylthiophene) *(pp. v, ix, xi, 4–11, 15–20, 22, 27–30, 35)*
**PCL** Polycaprolactone *(pp. 4, 6, 35)*
**Pd** Palladium *(p. 10)*
**PDT** Photodynamic Therapy *(p. 3)*
**PEG** poly(ethylene glycol) *(pp. 4, 35)*
**PTT** Phototermal Therapy *(p. 3)*

**ROS** Reactive Oxygen Species *(pp. 2, 3)*
**rpm** Revolutions per minute *(pp. 7, 8)*

**SBF** Simulated Body Fluid *(pp. xi, 12, 13, 23–25)*
**SEM** Scanning Electron Microscopy *(pp. 7, 10, 15, 16, 18, 30)*

**UV** Ultraviolet *(pp. v, vi, x, 2–4, 6–8, 11–13, 20, 22, 25, 27, 29, 30)*

**UVA** Ultraviolet A *(pp. 2, 3)*

**Vis** Visible *(pp. 3, 6–8, 12)*

# 1 Introduction

## 1.1 Motivation

The skin is the largest organ in the human body and executes numerous functions by virtue of its highly developed characteristics. It mainly acts as barrier between the external environment and the body, maintaining the internal conditions despite the external changes [2]. A skin wound leads to a breakage of this barrier and, as a result, to infections.

Chronic wounds are portrayed as an anomaly in the healing process, which can be divided in 3 stages, inflammation, tissue formation, and tissue remodeling. This anomaly arises from the delay of the previously mentioned stages [3]. Based on aetiology, chronic wounds can be classified as pressure, diabetic, venous and arterial insufficiency ulcers. Economically speaking this type of wounds lead to a burden in the healthcare system due to the need of specialised clinicians and the overall cost of the treatment. Furthermore, the patient undergoes notable physical and emotional discomfort [4].

Regarding the treatment of this ailment, it consists of tissue assessment and debridement, control of infection/inflammation, establishing moisture balance and managing wound exudate and observation of the wound edge. The employment of DDSs in patch form can be advantageous in this condition as it can provide a boundary between the environment and the body, maintaining the correct moisture, and supplying the necessary drugs with a lower periodicity [5].

The use of controlled drug release is advantageous in numerous situations, for example, to maintain drug concentration in the body within the therapeutic range during a larger time interval, reducing the probability of adverse side effects and the frequency of drug administration whilst improving the effectiveness of the treatment. Therewithal, the use of light as the stimuli to release the therapeutic agent brings an added value to the DDSs as it has a noninvasive nature, it's efficiently applied and has a high spacial and temporal control [6].

For the reasons stated above, the goal of this thesis is to study the benefits of light-responsive on-demand DDSs that use biocompatible and photosensitive materials, as it provides a barrier to protect the wounds and an efficient method to deliver the necessary

drug.

The research work described in this dissertation was carried out in accordance with the norms established in the ethics code of Universidade Nova de Lisboa. The work described and the material presented in this dissertation, with the exceptions clearly indicated, constitute original work carried out by the author.

## 1.2 Context

### 1.2.1 Stimuli Responsive Drug Delivery Systems

DDSs are described by J Rojo *et al*. [7] as "a formulation or a device that enables a therapeutic substance to selectively reach its site of action without reaching the nontarget cells, organs, or tissues". This systems can be managed through a variety of stimuli, internal and external.

Concerning the endo-stimuli-responsive DDSs, some of the variables that can activate the delivery of the drugs are the pH level, Reactive Oxygen Species (ROS) and enzymes [8].

Regarding the exo-stimuli-responsive DDSs, temperature, radiation, light, magnetic field and ultrasound are the main triggers of drug release [8]. The use of this class of stimuli proves to be beneficial as it provides a control over the duration and spacial extension in which the drug is released [9]. In 1.2.2 the light-responsive DDSs are discussed in detail.

### 1.2.2 Light-responsive DDSs

Light is an electromagnetic radiation that can be divided by its wavelength in to several categories, the ones relevant to this study are UV, visible and Near-Infrared (NIR). It can be used as a one time stimulus to release the drug it carries or as a switch, displaying the ability to activate or terminate the release in a dynamic system [9]. Taking into consideration the respective wavelength and tissue penetration of each light the Table 1.1 was organized.

Ultraviolet A (UVA) is the main component of the UV radiation that reaches the earth and causes many skin and eyes damages, it has the lower tissue penetration and range of wavelength and high phototoxicity resulting in low drug release [9].

The visible range of the light spectrum, between 400 and 650 nm, offers a variety of colors, easily seen by the human eye, and a tissue penetration between 0.5 and 2.5 mm.

NIR has a wavelength between 650 and 950 nm, displays low phototoxicity therefore being suitable for a variety of medical applications.

Table 1.1: Tissue Penetration of the different lights on the spectrum.

| Light | Wavelength | Tissue Penetration | Reference |
|---|---|---|---|
| UVA | 320–400 nm | 100–150 $\mu$m | [9] |
| Visible | 400–650 nm | 0.5-2.5 mm | [10] |
| NIR | 650–950 nm | 1–3.5 mm | [10] |

NIR Photoresponsive DDSs can be divided into 3 categories [10], as depicted in figure 1.1:

1. Photothermal responsive DDSs: nanomaterial-mediated Phototermal Therapy (PTT) under NIR laser irradiation to generate heat to destroy thermal-responsive materials, generally constructed via integrating thermal-responsive components into nanomaterials containing drugs and photothermal agents (organic dyes, such as indocyanine green, and organic nanoparticles;

2. Photodynamic responsive DDSs: rely on photosensitizer mediated Photodynamic Therapy (PDT) to allow NIR triggered drug release, PDT utilizes photosensitizers and light irradiation to generate ROS;

3. Photoconversion responsive DDSs: are fabricated through integrating UV/Visible (Vis) light-sensitive components into upconverting nanosystems with loadings of drugs. Under NIR laser irradiation, upconversion materials convert NIR light into UV/Vis light that can destroy these sensitive moieties, allowing for on-demand drug release.

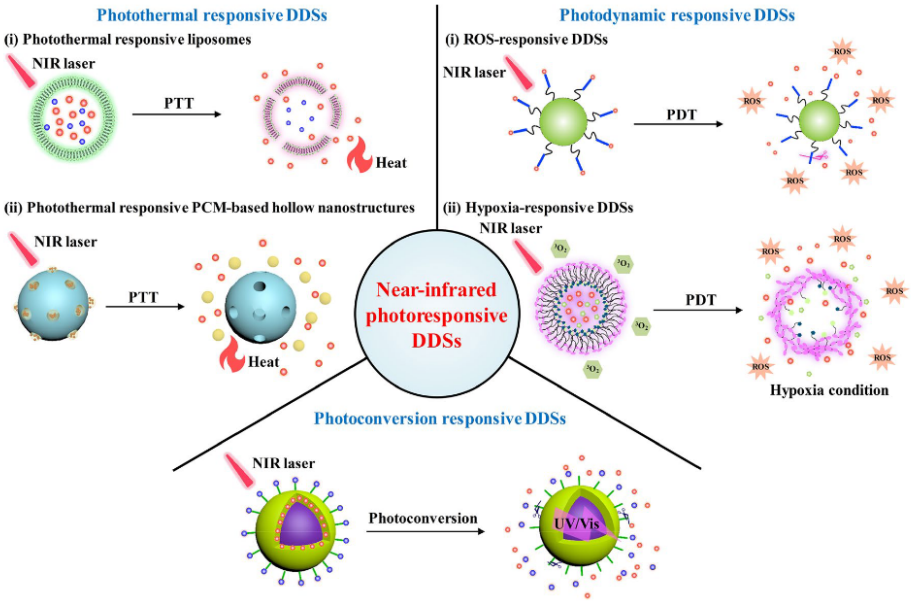


Figure 1.1: Illustrative representation of NIR photoresponsive DDSs [10].

## 1.3 State of the Art

Light-responsive DDSs have gained significant attention in recent years as they offer the potential for targeted and controlled drug release in response to light stimuli. In the field of dermal drug delivery, light-responsive systems have shown promise in improving treatment efficacy, reducing side effects and achieving localized drug delivery [6].

One approach to achieving light-responsive drug delivery is through the use of photoresponsive hydrogels. These hydrogels can undergo reversible changes in their physical and chemical properties in response to light, allowing for the controlled release of drugs in response to specific wavelengths of light. Examples of photoresponsive hydrogels include azobenzene (photosensitizer) and poly(ethylene glycol) (PEG) hydrogel developed by [11], this system showed reversible photoisomerization and volume changes when exposed to specific wavelengths of UV radiation and silicone, spiropyran and merocyanine hydrogels where, after UV irradiation the hydrophobic spiropyran transforms into the hydrophilic merocyanine releasing the doxorubicin content [12].

Recently, nanomaterials such as gold nanoparticles have also been explored as potential light-responsive drug delivery platforms due to their unique optical properties and high antimicrobial activity. Gold nanoshell-coated chitosan liposomes are used to deliver therapeutic agents after a pH or NIR stimuli [13].

Fibers made of polymeric and photosensitive compounds are also commonly used in this systems since a dermal patch can be made out of this filaments. [14] developed Polycaprolactone (PCL) and P3HT fybers that, when stimulated by light, encouraged the regeneration of tissue.

Using the polymer CA, [15] developed electrospun membranes that released a model drug, in this case Ibu, when a certain potential was applied. With this study it was verified that CA is a good base polymer to incorporate the model drug into. In [16] this polymer mixed with polyethylene oxide and methylene blue were able to, when exposed to radiation, produce reactive oxygen species, which lead to the creation of hypoxia conditions, preventing the development of bacteria.

Despite the promising results demonstrated by light-responsive DDSs, there are still challenges that need to be addressed, such as the optimization of drug release kinetics, ensuring biocompatibility, and achieving effective penetration of light through the skin.

The systems mentioned above have been compiled into the table I.1 in Appendix I.

Taking into account the DDSs already produced, this thesis will provide an innovative contribution to the development of light responsive DDSs for dermal applications by introducing a DDSs with materials never assembled together, CA, P3HT and Ibu, taking advantage of their unique properties, such as the photosensitivity of the P3HT.

With that intention, a set of goals must be accomplished, particularly, this work is divided in 3 main objectives:

1. Production of CA fibers using conventional electrospinning to incorporate a model

drug;

2. Incorporation of P3HT using two distinct approaches: (i) direct introduction of the photosensitive polymer into the CA/Ibu solution (configuration referred to as 'blend'); and (ii) coating the CA/Ibu membrane with P3HT using the electrospray technique (configuration referred to as 'spray').;

3. Evaluation of the drug release under different radiations.

Taking into mind the aforementioned thesis aims, an introduction to the procedures and materials to be employed will be presented next.

The fiber producing technique used is electrospinning, it produces fibers with diameters in the range of submicron to nanometer. Electrospun fibers have several advantages such as high surface area to volume ratio, pliability, mechanical performance, processing simplicity, and relatively low cost making them attractive to several applications including in the biomedical field [17, 18].

On the list of materials utilized, the first one is CA which is obtained by the acetylation of cellulose [19]. It offers a variety of advantages as it overcomes the poor solubility of its precursor compound and grants numerous beneficial features such as biocompatibility, environmentally well-disposed attributes, inexpensive and non-toxic, therefore being used for DDSs, particularly transdermal and wound dressing patches [18, 19]. To be used in electrospinning CA was dissolved in acetone and dimethylacetamide [17].

P3HT, is a semiconducting polymer recognized by its optoelectronic properties, in particular, its photosensitivity [20], such characteristics stem from its ability to crystallize [21].

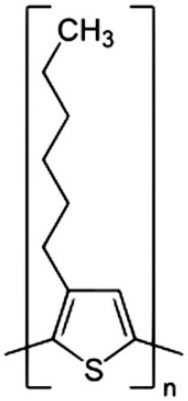


Figure 1.2: Chemical structure of P3HT [22].

In figure 1.2 the chemical structure of the polymer is represented. Regrettably P3HT is unable to form nanofibers through electrospinning on account of deprivation of chain entanglement, thus the necessity of blending this substance with another polymer [14], or using the electrospray process to deposit it.

On the other hand, P3HT-PCL fibers have been explored and [20] came to the conclusion that this blend is biocompatible and cells can attach to the surface of this fibers. Additionally, owing to its photosensitive features it's an ideal material to be used for photocurrent therapy, which is a combination of electrotherapy and phototherapy, regarding the first, the production of electrons from the photosensitive polymer being irradiated creates a electromagnetic field which stimulates the cells to proliferate and encourages nucleotide synthesis and in the second therapy mentioned, direct light stimulation also has the same cellular proliferation effect. Due to the enhancement of cell multiplication and consequent decrease in healing time the use of P3HT in photocurrent therapy is beneficial for tissue regeneration.

Ibu is an anti inflammatory and antipyretic commonly prescribed as it bears all the benefits of other therapeutics, like Aspirin, without such aggravated side effects, for example, nausea, vomiting and gastric irritation [23]. Figure 1.3 represents the chemical structure of the medication in question.

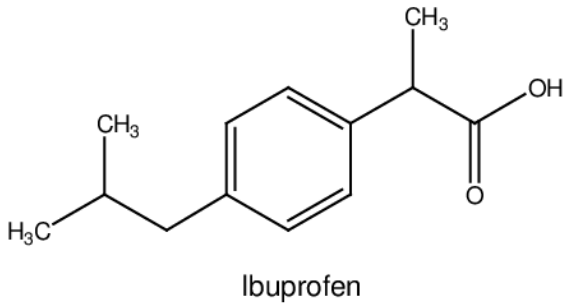


Figure 1.3: Chemical structure of Ibuprofen [24].

The previously described therapeutic was chosen as the model drug for this study as it possesses a specific absorbance value of 222 nanometers [25] which will be used to determine if the Ibu was released resorting to UV/Vis spectroscopy.

# 2

# Materials and Methods

In order to produce light-responsive DDSs for dermal applications a photosensitive compound (P3HT), biocompatible polymer (CA) and model drug (Ibu) nanofibers must be produced.

In this chapter a brief description of the fabrication methods and characterization techniques is provided. The chosen method of production is conventional electrospinning and electrospray. The characterization techniques are Scanning Electron Microscopy (SEM), Fluorescence Microscopy and Spectroscopy, UV/Vis Spectroscopy and Current-Voltage Characteristic Curve (I-V Curve).

## 2.1 Fiber Production using the electrospinning technique

In this section, the fiber setups, solutions and production techniques chosen will be discussed.

### 2.1.1 Preparation of polymeric solutions

#### 2.1.1.1 CA solution

The prepared solution contains 12% (w/v) of CA (Mn ~ 50.000 with 40% of acetyl groups, Sigma Aldrich) dissolved in a 2:1 proportion of acetone (Honeywell Riedel-de Haën, 99.5%) and Dimethylacetamide (DMAc) (Carlo Erba Reagents S.A.S.). The solution dissolved with constant magnetic agitation of 100 Revolutions per minute (rpm) at room temperature for approximately 24 hours, after which it was homogeneous as it didn't present any suspended particles.

#### 2.1.1.2 CA and Ibuprofen solution

The CA and Ibu solution was prepared as the CA solution above mentioned, the difference relies on the use of 10% (w/v) of CA, that was reduced to ensure minimal variation in the viscosity of the solution, and the addition of 0.2% (w/v) of Ibu (Farma-Quimica Sur S.L., 99.3%).

#### 2.1.1.3 P3HT solution

The solution contains 0.5% (w/v) of P3HT (Ossila, 95.2% RR) dissolved in chlorobenzene (Sigma-Aldrich, 99.8%) and 8% (w/w) acetonitrile (Honeywell Riedel-de Haën, 99.9%). The solution was dissolved with constant magnetic agitation of 100 rpm at room temperature and humidity for approximately 16 hours.

#### 2.1.1.4 CA, Ibuprofen and P3HT solution

In this solution, the same concentrations of CA and Ibu were used, 10% (w/v) of CA and 0.2% (w/v) of Ibu, the amount of P3HT used was 0.5% (w/v). This solution was dissolved in a blend of Dichloromethane (DCM) (Carlo Erba Reagents S.A.S) and acetone in a 1:1 (v/v) proportion in order to produce fibers of similar diameter as the ones produced from the solution in section 2.1.1.2 [26] and because a solvent for P3HT was necessary as neither DMAc nor acetone perform well in the dissolvement of the mentioned polymer, in this case DCM settles this issue [27]. The solution dissolved with constant magnetic agitation of 100 rpm at room temperature and humidity for approximately 36 hours.

### 2.1.2 Selected fiber setups

In order to study the release of Ibu when irradiated with UV/Vis light two setups were selected. The first, represented in the left segment of figure 2.1, has a spray setup in which the inside has a blend of CA and Ibu, and the outer shell is a thin layer of P3HT, made with the electrospray technique. The second setup, on the right of figure 2.1, is a blend of the three materials above mentioned.

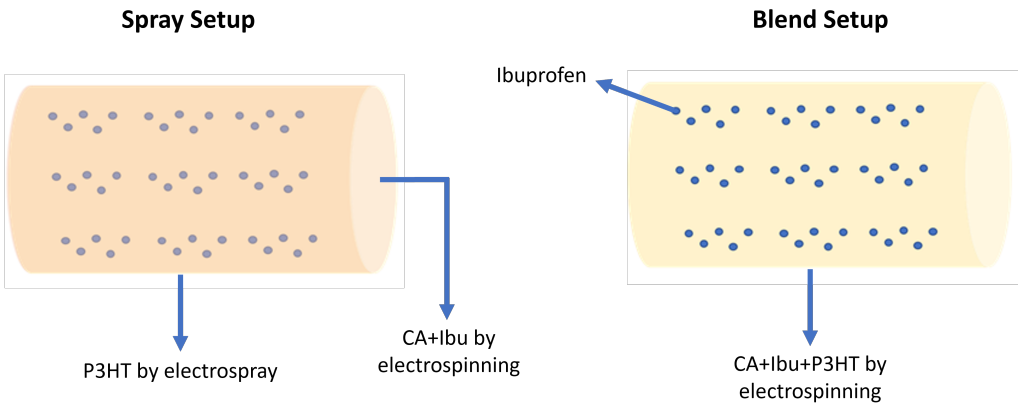


Figure 2.1: Selected fiber setups to evaluate the release of Ibuprofen. The blue circles represent the Ibuprofen that was incorporated. The left diagram has a different colour and the colour of the blue circles is faded in order to represent that a layer of P3HT was deposited on top of the CA+Ibu membrane.

### 2.1.3 Electrospinning

In order to produce fibers from the solutions previously described the experimental details represented in figure 2.2 was employed.

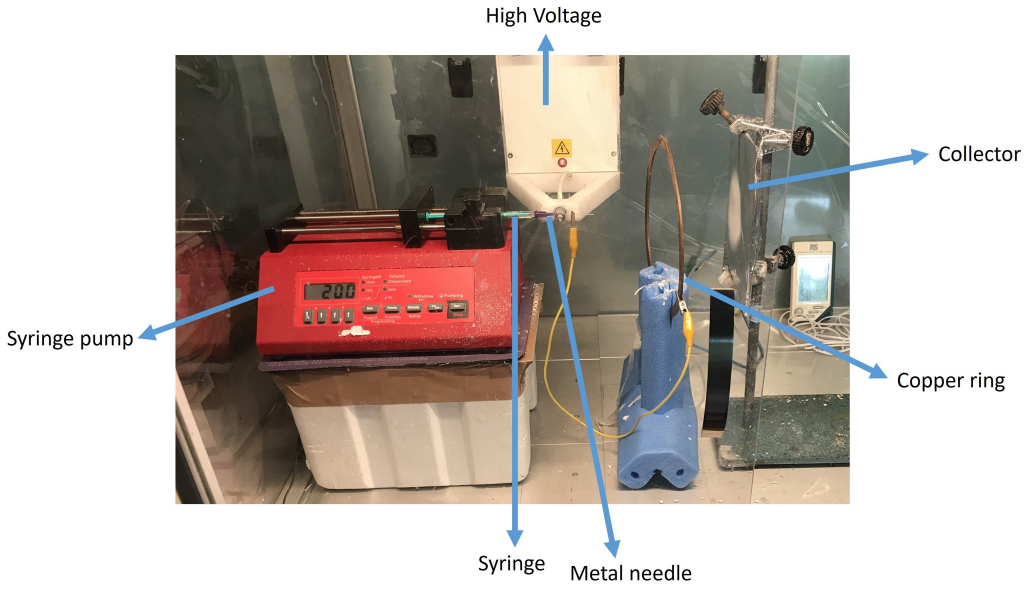


Figure 2.2: Experimental setup of the electrospinning process.

A 1 mL syringe (Injekt, B.Braun) with a metal needle (Iberiana Technical), with an inner diameter of 0.51 mm, was placed in a syringe pump (model 100 series, Kd. Scientific) in order to eject the polymeric solution at a constant rate while a high voltage (using a Keithley 237 High Voltage Source Measure Unit) is being applied between the needle and a collector connected to the ground. A copper metal ring was also placed to homogenize the electric field and, consequently, allow greater directional control of the fibers towards the collector. The specific parameters used for each solution are available in table 2.1.

### 2.1.4 Electrospray

Electrospray is a technique similar to electrospinning, it is guided by the same principle and uses the same setup. The feature that distinguishes the two techniques is the use of a low viscosity solution in electrospray, which results in the production of particulate products (nanoparticles or microparticles) as opposed to fibrous ones [28], this proves to be advantageous when in need to deposit a layer of a polymer with the inability of chain entanglement, like P3HT.

To produce the layer of P3HT the experimental setup was the same as in figure 2.2 with some modifications such as a needle with inner diameter of 0.20 mm and the copper ring was not used.

Table 2.1 contains a synopsis of the process parameters necessary to produce electrospun fibers and the layer of P3HT with electrospray.

Table 2.1: Parameters for the production of membranes of CA, CA and Ibuprofen, CA, Ibuprofen and P3HT, by electrospinning, and layer of P3HT by electrospray.

| Parameters | CA | CA+Ibu | CA+Ibu+P3HT(blend) | P3HT |
|---|---|---|---|---|
| Syringe diameter (mm) | 4.5 | 4.5 | 4.5 | 4.5 |
| Flow Rate (mL/h) | 0.2 | 0.2 | 1 | 0.1 |
| Needle Caliber | 21G | 21G | 21G | 27G |
| Distance needle to target (cm) | 15 | 15 | 13 | 13 |
| Copper ring | Yes | Yes | Yes | No |
| Voltage (kV) | 20 | 20 | 15 | 15 |
| Deposition interval (h) | 8 | 8 | 2 | 8 |
| Temperature (ºC) | 20-25 | 20-25 | 20-25 | 20-25 |
| Humidity (%) | 30-50 | 30-50 | 30-50 | 30-50 |

## 2.2 Characterization techniques

### 2.2.1 Scanning Electron Microscopy

SEM is a characterization technique used to evaluate the morphology and defects in substances using a high energy electron beam to scan the uppermost layer of the materials.

For the conducted study, samples with dimensions of approximately 0.5 cm by 0.5 cm were cut from different types of membranes and fixed using a conductive carbon tape on the sample holder disk, finally, all samples were coated with a thin layer of Gold (Au)-Palladium (Pd). Membranes of CA, CA+Ibu, CA+Ibu+P3HT(spray) and CA+ibu+P3HT(blend) were evaluated, for the last two types, analysis was performed before and after drug release.

The S2400 Hitachi model was employed for conducting the technique, and the resulting images were analyzed using image processing software (ImageJ®, NIST) to analyse the average fiber diameters.

### 2.2.2 Optical Microscopy

Optical Microscopy is a widely used imaging technique that utilizes visible light to magnify and visualize microscopic structures of various materials [29].

The samples were placed on a glass microscope slide (Deltalab S.L.), which was inserted into the corresponding holder of the inverted optical microscope of the Leica brand, model DMi8. The images were acquired in reflection mode and captured at magnifications of 50x, 100x, or 200x. Membranes of CA, CA+Ibu, CA+Ibu+P3HT(spray) and CA+ibu+P3HT(blend) were analyzed.

### 2.2.3 Fluorescence Microscopy

The fluorescence microscope's objective is to separate excitation and emitted light. This is typically accomplished with optical filters, and the choice of these filters in relation to the used indicators is the key to successful imaging [30].

This technique was used to verify the photoluminescence of P3HT. The microscope used is the same as in section 2.2.2 and has three different filters available, their characteristics are presented in table 2.2.

Table 2.2: Fluorescence filters characteristics. The filter names are linked to the fluorochrome utilized within the filter. The DAPI, or 4',6-diamidino-2-phenylindole, filter, the green fluorescent protein (GFP) filter and the rhodamine (RHOD) filter are used to evaluate the photoluminescence of the P3HT.

| Filter | Excitation (nm) | Dichroic (nm) | Emission (nm) | Emission Colour |
|---|---|---|---|---|
| DAPI | PB 350/50 (UV) | 400 | PB 460/50 | Blue |
| GFP | PB 470/40 (Blue) | 495 | PB 525/50 | Green |
| RHOD | PB 546/10 (Green) | 560 | PB 585/40 | Orange (rhodamine) |

### 2.2.4 Fluorescence Spectroscopy

Fluorescence spectroscopy is a non-destructive analysis that allows recording emission and excitation spectra of samples. This method was used to verify the presence of P3HT. The excitation spectrum corresponds to the fluorescence intensity as a function of the excitation wavelength, while keeping the emission wavelength constant. On the other hand, the emission spectrum, acquired in this study, represents the fluorescence intensity as a function of the emission wavelength, while keeping the excitation wavelength constant [31].

To obtain the emission spectra of the CA, CA+Ibu, CA+Ibu+P3HT(spray), CA+Ibu+P3HT (blend) membranes and of a P3HT covered aluminium foil, the Pack Fluorescence FLEX CUV equipment (Sarspec) was used, which allows fluorescence measurements from UV to NIR. The UV excitation laser has a wavelength of 365 nm, and the higher intensity setting was used. The equipment also has a bandpass filter (cutoff at 410 nm) to reduce the contribution of the incident beam radiation.

This analysis was performed in order to investigate the fluorescence characteristics of the membranes, to determine the radiation emitted by the samples when excited by UV radiation.

### 2.2.5 Current-Voltage Characteristic Curve

I-V Curve is a graphical representation that shows the relationship between the current flowing through a device and the voltage applied across it.

The curves will be used to obtain the conductivity of the membranes when exposed to different radiations, UV, infrared, white light, ambient light and in the dark, to evaluate if the material is photoconductive/photosensitive.

The process of conductivity measurement is carried out using a pico-ammeter/voltage source (model 6400, Keithley Instruments), two probe tips (Alessi REL450), and the

values of current-voltage (I-V) were recorded with the assistance of a computer. Planar conductivity is measured on the membrane's surface, and for this purpose, a carbon conductive ink (Bare Conductive®) was used to create rectangular-shaped electrodes measuring 5 mm by 3 mm, with a 2 mm separation between them.

In section I.2 of Appendix I can be found a more complete explanation of this technique.

## 2.3 Drug Release Study

### 2.3.1 Simulated Body Fluid

SBF is an isotonic solution that maintains the pH of solutions, is non-toxic, and simulates the inorganic part of blood plasma.

In order to prepare this solution the procedure described by Kokubo *etal* [32] was used.

Table 2.3: Reagents used to prepare the SBF solution.

| Reagent | Ions | Quantity (g/mL) | Brand |
|---|---|---|---|
| NaCl | $Na^+$; $Cl^-$ | 6,547 | *Sigma-Aldrich* |
| $NaHCO_3$ | $Na^+$; $HCO_3^-$ | 2,268 | *PanReacAppliChem* |
| KCl | $K^+$; $Cl^-$ | 0,373 | *Scharlau* |
| $Na_2HPO_4 \cdot H_2O$ | $Na^+$; $HPO_4^{2+}$ | 0,178 | *FLuka Analytical* |
| $MgCl_2 \cdot {}_6H_2O$ | $Mg^{2+}$; $Cl^-$ | 0,305 | *PanReacAppliChem* |
| 1M HCl | $H^+$; $Cl^-$ | 15 | —— |
| $CaCl_2 \cdot {}_2H_2O$ | $Ca^{2+}$; $Cl^-$ | 0,368 | *Sigma-Aldrich* |
| $Na_2SO_4$ | $Na^{2+}$; $SO_4^{2+}$ | 0,071 | *Sigma-Aldrich* |
| $(CH_2OH)_3CNH_2$ | —— | 6,057 | *Sigma-Aldrich* |
| 1M HCl | $H^+$; $Cl^-$ | until it reaches a pH of 7,4 | —— |

The reagents listed in table 2.3 were added to 700 $mL$ of ultrapure water in that respective order and with constant agitation. Afterwards the solution was heated until it reached 37ºC and finally the necessary volume of water was added to reach 1000 $mL$. This solution must be stored in a refrigerator at 5ºC.

### 2.3.2 Ultraviolet/Visible Spectroscopy

This technique was used in order to obtain the absorbance spectra of several solutions being tested using a UV/Vis spectrophotometer (T90+ UV/VIS Spectrometer PG Instruments Ltd).

With the use of a graphic relating the absorbance with concentration (calibration curve), a linear relation is obtained due to the Lambert-Beer's Law, which can be used to estimate the amount of substance, ibuprofen, released from the fibers previously produced [33].

### 2.3.3 Ibuprofen calibration curve

To conduct the drug release study, the absorption-concentration calibration curves were first created using the following methodology: SBF+Ibu and $H_2O$+Ibu solutions with a concentration of 20 mg/L were prepared, dilutions were made to obtain different concentrations, from 0.5 mg/L to 20 mg/L, following that, the absorbance spectrum of each concentration was acquired.

### 2.3.4 Study of the release medium

In order to study the appropriate medium for the drug releases the same amount (10 mL) of four solutions (SBF+Ibu, $H_2O$+Ibu, SBF and $H_2O$) were submitted to UV light (IP66 model, 100 W, 365 nm wavelength light-emitting diode) while their absorbance level was evaluated in regular time intervals, clarified in table 2.3a. The experimental setup pictured in figure 2.3b was used.

(a)

| Total release time (min) | | | | | | | | | | | |
|---|---|---|---|---|---|---|---|---|---|---|---|
| 0 | 2 | 4 | 6 | 8 | 10 | 12 | 22 | 32 | 52 | 72 | 92 |

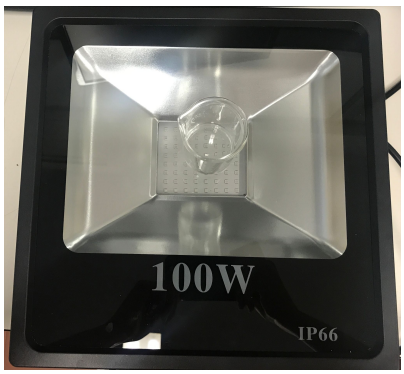


(b)

Figure 2.3: (a) Total release time for the medium study; (b) Experimental setup for the medium study

### 2.3.5 Drug release from the membranes

The membranes were submitted to active and passive drug release tests.

In the passive drug release test, the membranes were submerged in 5 mL of $H_2O$ for a total of 9 days and their absorbance level was measured in regular time intervals.

In the active tests, the membranes are also submerged in 5 mL of $H_2O$ and subjected to UV light, setup in figure 2.3b and infrared light (230 V, 60W), figure 2.4, for a total duration of 112 minutes.

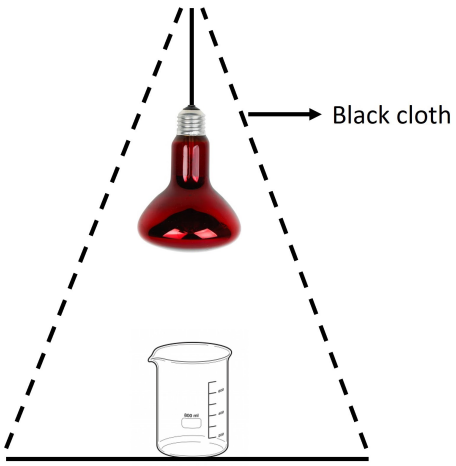


Figure 2.4: Experimental setup for infrared active drug release test.

# 3

# Results and Discussion

The obtained results will be presented and discussed in this chapter. First, the membranes produced by electrospinning and electrospray will be presented and a morphological and electrical analysis of each membrane will be conducted, afterwards, the drug release tests results will be showcased.

## 3.1 Membrane Production

### 3.1.1 Morphological Analysis

In this subsection, a morphological analysis of all the membranes produced will be delivered, making use of different techniques such as SEM, optical microscopy, fluorescence microscopy and spectroscopy.

#### 3.1.1.1 Macroscopic Aspect

In this study two membranes with P3HT incorporated were studied. The first one, called CA+Ibu+P3HT(spray) is made by electrospray of a P3HT solution over a CA+Ibu membrane, while the second, CA+Ibu+P3HT(blend) is made by electrospinning of a solution with three components, CA, Ibu and P3HT. The second one is a more common method utilized to create fibers but, in an effort to use less amount of the photosensitive polymer, due to its cost, and to evaluate the difference in drug release of this optic membrane if the polymer is only present in the surface of the membrane, the first membrane was developed.

By observation of figure 3.1 we can see that the images 3.1a, 3.1b and 3.1d are all very similar, the last one, that has P3HT incorporated, should reflect more of the characteristic colour of this polymer yet, it doesn't, mainly do to the low concentration of said compound. Regarding figure 3.1c, the electrospray of P3HT seems to be irregular and the solution would spread and deposit more on the target then on the membrane. To understand why it didn't disperse in a homogeneous way various test were performed, the one that lead to a conclusion was the electrospray of a CA+Ibu film where the solution deposited uniformly in the film, with this test we concluded that the membrane was absorbing the

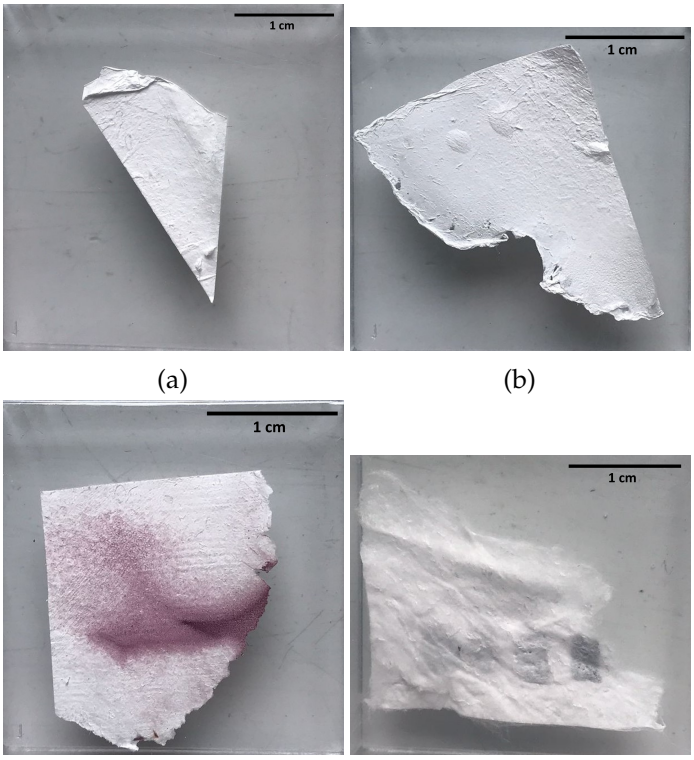


Figure 3.1: Visual aspect of the four different membranes produced: 3.1a - CA membrane, 3.1b - CA+Ibu membrane, 3.1c - CA+Ibu+P3HT(spray) membrane and finally 3.1d - CA+Ibu+P3HT(blend) membrane.

solution and because of that only some areas are strongly pigmented but all the membrane has P3HT.

#### 3.1.1.2 SEM

In order to obtain the value of Mean Fiber Diameter (MFD) for each type of membrane produced the image processing software ImageJ® was used, performing 30 random measurements per membrane in the highest magnification image.

The figure 3.2a represents a SEM image of the CA membranes. This image highlights the randomness of fiber directions as well as a relatively high distribution of fiber diameters, 505±196 nm, 3.2b. This membrane was produced following the same electrospinning parameters of previous studies and obtained a similar MFD [15].

The same process was conducted in the CA+Ibu membranes, represented in figures 3.3a and 3.3b. These membranes present a lower MFD, 336±169 nm, than the CA membranes, the latter membranes were made with a solution containing 12% (m/v) of CA, while the first were made with 10% (m/v), given this difference in the polymer concentration in the solutions, and knowing that the rise of this concentration increases the diameter of the fibers [28], the reduction of the MFD is justified. Figure 3.3a reveals some non-uniform and beaded fibers which cause can be the uneven incorporation of Ibu, due to the small

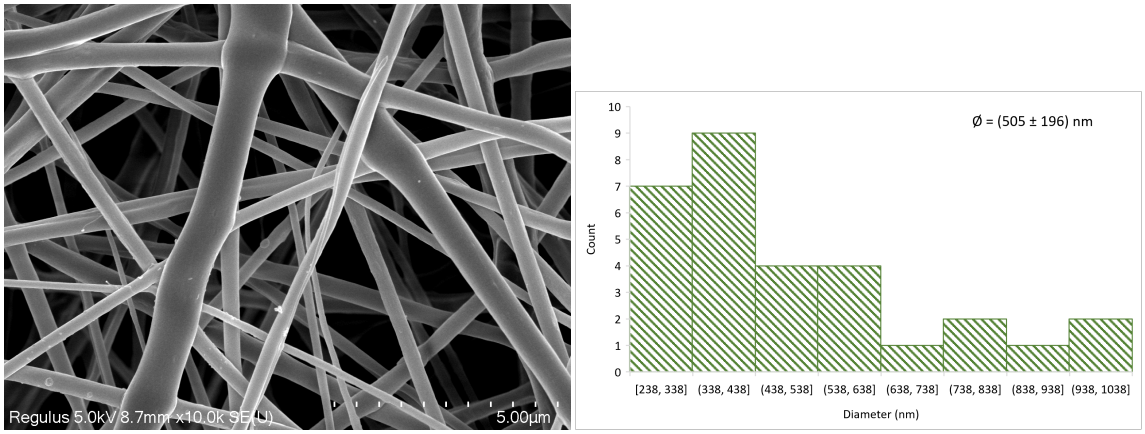


(a) (b)

Figure 3.2: SEM image of CA fibres (a) and respective histogram with MFD (N=30) (b). Scale bars represent 5 µm.

amount present in the solution.

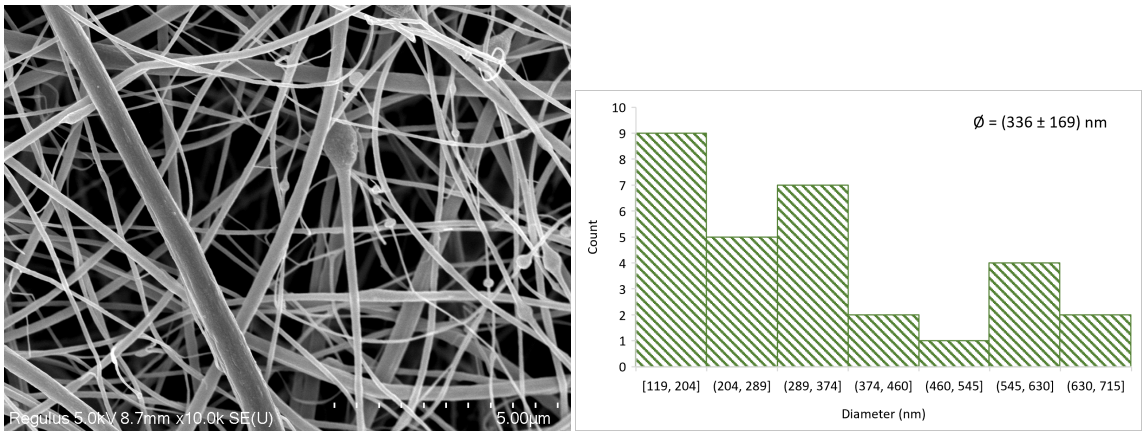


(a) (b)

Figure 3.3: SEM image of CA+ibu fibres (a) and respective histogram with MFD (N=30) (b). Scale bars represent 5 µm.

Regarding the CA+Ibu+P3HT(spray) membranes, the technique of electrospray, used to deposite the P3HT, isn't commonly used in the development of this type of fibers thus, literature evaluating the properties of similar membranes was not found.

The MFD of this fibers is 816±664 nm, which is much higher than the values of the previously described membranes due to the incorporation of the P3HT particles in the already present CA+Ibu fibers. Figure 3.4a reveals some fused fibers, which can be justified by changes in the ideal humidity and temperature parameters during the electrospinning process, these changes can affect the viscosity of the solution but, more importantly, alter the solvent evaporation rate, thus leading to the formation of non-uniform and defective fibers [28]. Another reason for the existence of this fused fibers is the accumulation of P3HT in between them, creating a fiber with irregular diameter.

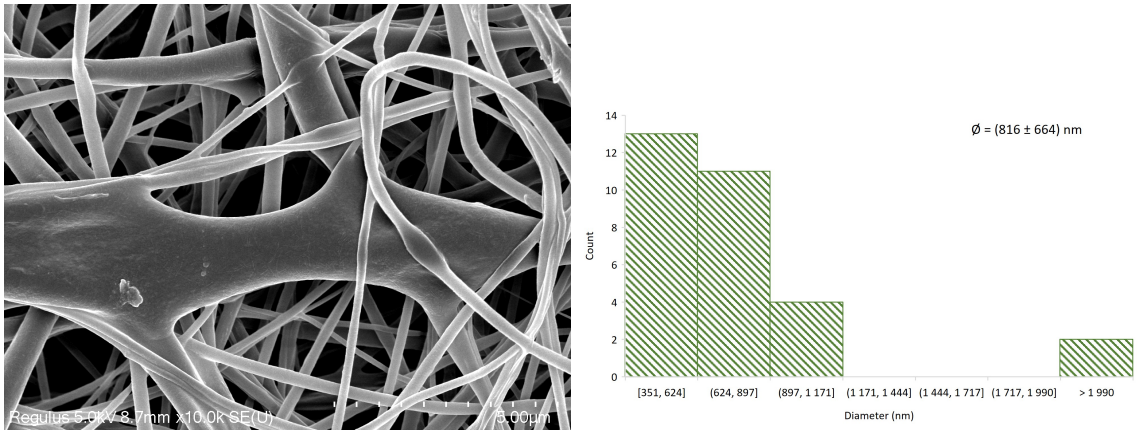


(a) (b)

Figure 3.4: SEM image of CA+ibu+P3HT(spray) fibres (a) and respective histogram with MFD (N=30) (b). Scale bars represent 5 µm.

In figure 3.5a the SEM image of the CA+Ibu+P3HT(spray) membrane after drug release is depicted. The membranes were evaluated after drug release in order to understand if this procedure affected the MFD and the overall appearance of the fibers. In figure 3.5b the diameter of 30 randomly selected fibers is represented in a manner that illustrates the variation in the diameter of the fibers, the MFD is 539±174 nm, when comparing this value to the value of the CA+Ibu+P3HT(spray) membrane that did not undergo drug release, it can be inferred that the MFD has decreased a significant amount. This phenomenon is attributed to the release of ibuprofen into the surrounding medium.

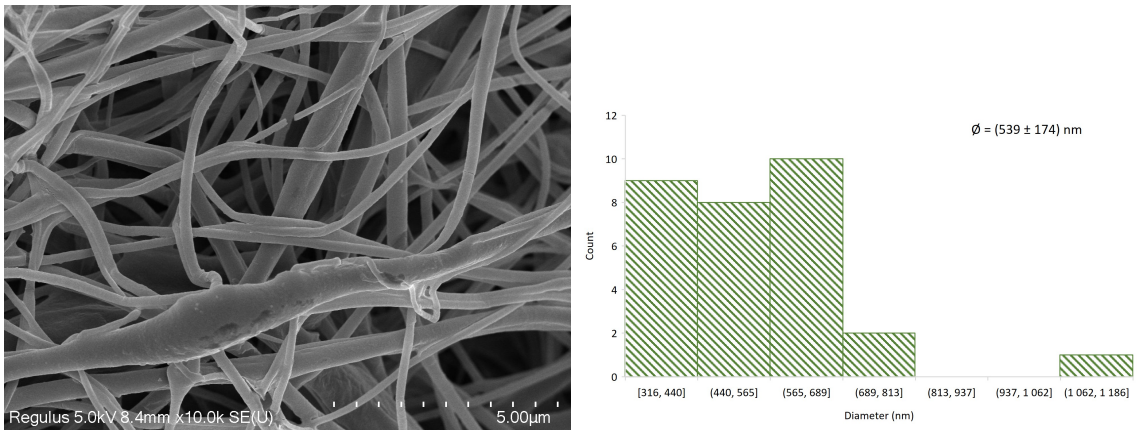


(a) (b)

Figure 3.5: SEM image of CA+ibu+P3HT(spray) fibres after drug release (a) and respective histogram with MFD (N=30) (b). Scale bars represent 5 µm.

Looking at figure 3.6, which is related to the CA+Ibu+P3HT(blend) membrane we can see that this fibers present a much higher MFD than the previously analysed fibers, with a value of 1788±850 nm. Knowing that the article [26] this membrane was based only used CA and didn't incorporate the drug and photosensitive compound, and that both

increased the viscosity of the solution, it was expected to observe some difference in the MFD of this membrane, regarding the shape of the fibers, it is as expected a ribbon-like structure due to the use of a high volatile solvent, DCM [26]. The inability to control the environmental conditions, namely the temperature and humidity also influence the results obtained. However it is a successful experiment as it was possible to produce fibers with this composition.

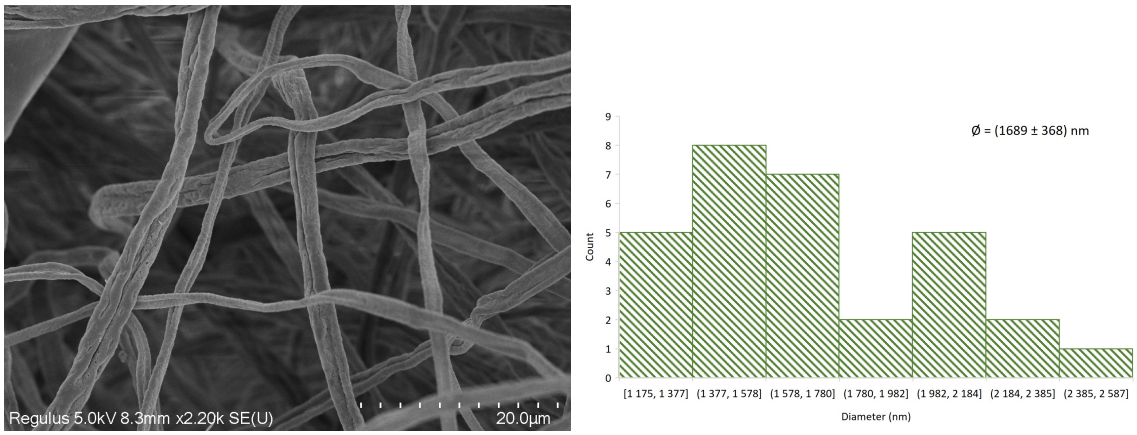


(a) (b)

Figure 3.6: SEM image of CA+ibu+P3HT(blend) fibres (a) and respective histogram with MFD (N=30) (b). Scale bars represent 20 µm.

Finally, by observation of figure 3.7, which corresponds to the CA+Ibu+P3HT(blend) membrane after drug release, we can verify the same ribbon-like shape as previously described and the MFD value is 1689±368 nm, from this we can concluded that there is a decrease of the MFD after release but a not so drastic one has seen in the CA+Ibu+P3HT(spray) membrane.

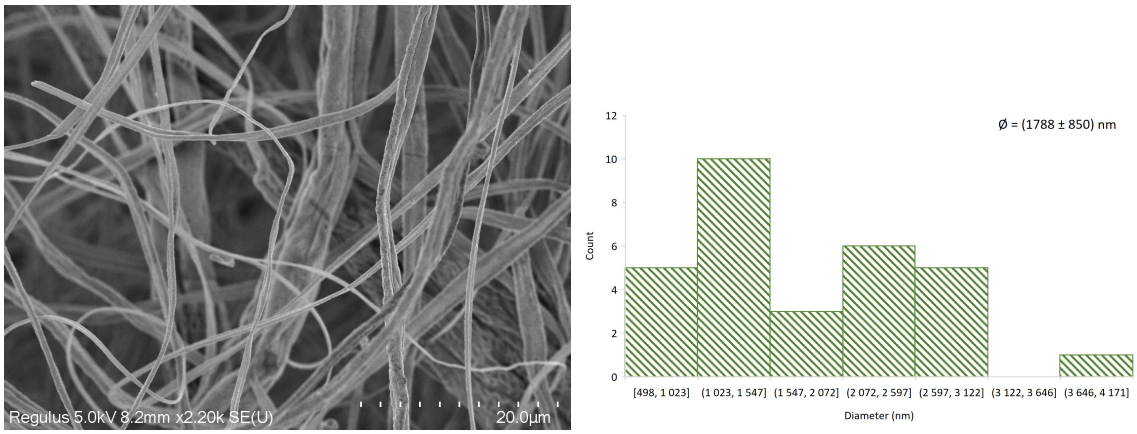


(a) (b)

Figure 3.7: SEM image of CA+ibu+P3HT(blend) fibres after drug release (a) and respective histogram with MFD (N=30) (b). Scale bars represent 20 µm.

#### 3.1.1.3 Fluorescence Microscopy

The photoluminescence of the various membranes was evaluated by Fluorescence Microscopy. The microscope used allows the observation of samples through fluorescence cubes, with the DAPI filter corresponding to UV excitation, GFP to blue light excitation, and RHOD to green light excitation. These filters are used because they allow for the specific detection and visualization of different structures, molecules, or proteins within a sample. The images in this section were acquired using a 100x magnification.

Observing figure 3.8, it is possible to verify that the CA+Ibu+P3HT membranes possess more fluorescence intensity than the other membranes evaluated, which was expected since P3HT is the only compound in the membranes that is capable of light emission. Between the two membranes with P3HT integrated, the membrane with this compound blended in to the solution and then put through electrospinning possesses more fluorescence intensity than the electrosprayed one, mainly in the GFP filter, a reason for this is that the P3HT distribution in this membrane is more homogeneous than in the electrosprayed membrane.

#### 3.1.1.4 Fluorescence Spectroscopy

To investigate the fluorescence characteristics of the membranes, Fluorescence Spectroscopy analysis was performed to determine the radiation emitted by the samples when excited by UV radiation with a wavelength of 365 nm. The maximum intensity of the beam was used to perform this test in the CA, CA+Ibu, CA+Ibu+P3HT(spray), CA+Ibu+P3HT(blend) membranes and in a P3HT covered aluminium foil, the last sample mentioned was used to verify that the peaks observed relate to the photoluminescent compound present in the membranes.

There is a band pass filter with a cutoff frequency of approximately 410 nm to reduce the amount of measured signal from the excitation source. As a consequence, artifacts appear in the measured spectra: a peak at 420 nm, still originating from the excitation radiation and accentuated by the abrupt cutoff caused by the filter, and another less pronounced peak at 840 nm, corresponding to a harmonic of the previous artifact.

Analysing the curves in figure 3.9, we can see that P3HT, the dark blue curve, has peaks at 560 and 690 nm, according to the literature, the relevant peak is at 690 nm [34], so that wavelength is the one to consider.

Analysing the membranes without P3HT, specifically the light blue and orange curves corresponding to CA and CA+Ibu membranes, respectively, they exhibit relatively low emission intensity. This observation aligns with the fact that these membranes lack components with inherent fluorescence capabilities.

In contrast, regarding the membranes containing P3HT, namely the gray curve representing the CA+Ibu+P3HT (spray) membrane and the yellow curve representing the CA+Ibu+P3HT (blend) membrane, both present around the same level of intensity, lower than the P3HT sample and higher than the CA and CA+Ibu membranes.

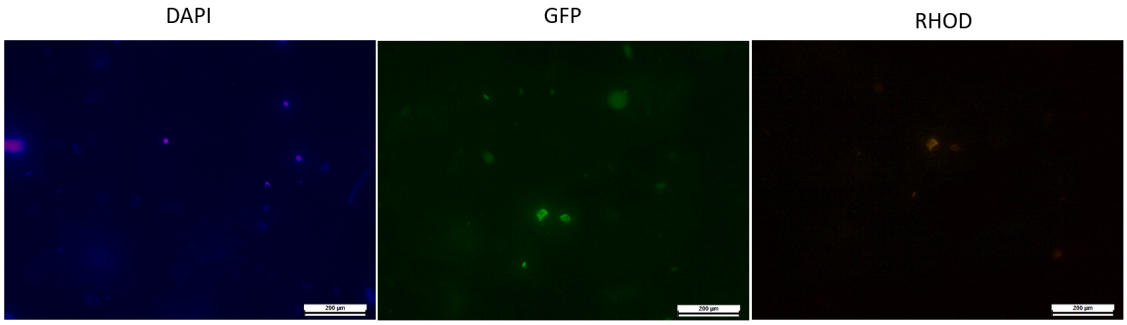


(a) CA membrane.

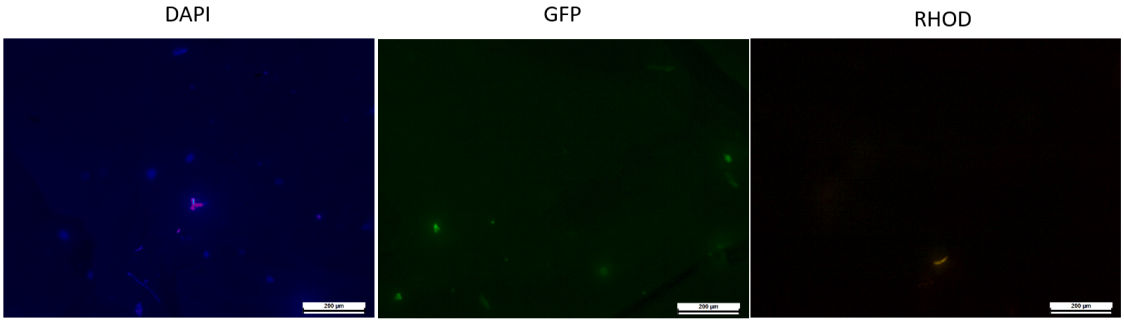


(b) CA+Ibu membrane.

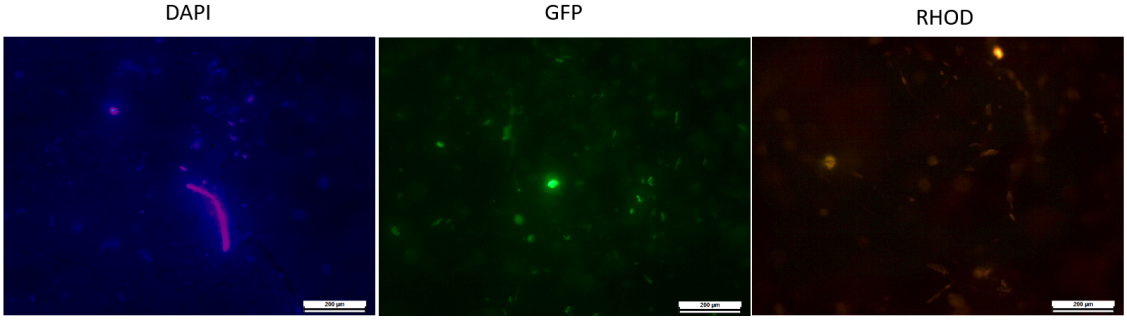


(c) CA+Ibu+P3HT(spray) membrane.

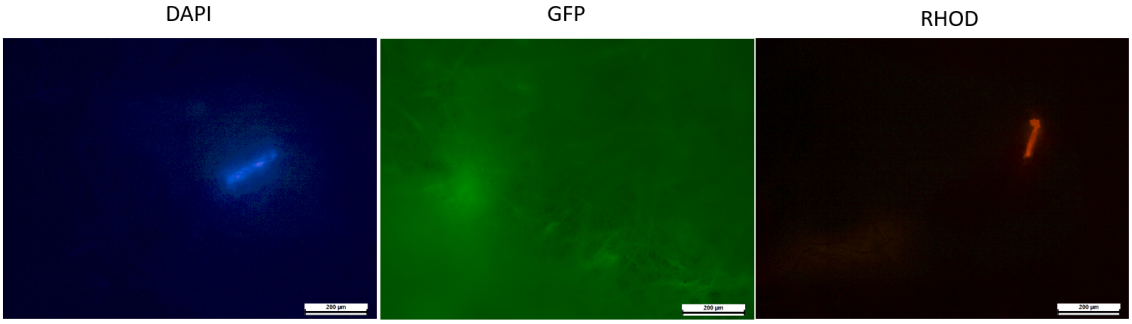


(d) CA+Ibu+P3HT(blend) membrane.

Figure 3.8: Fluorescence microscopy images of CA, CA+Ibu and CA+Ibu+P3HT membranes using the three different cubic filters, DAPI - 350 nm; GFP - 470 nm; RHOD - 546 nm. Scale bar represent 200 µm.

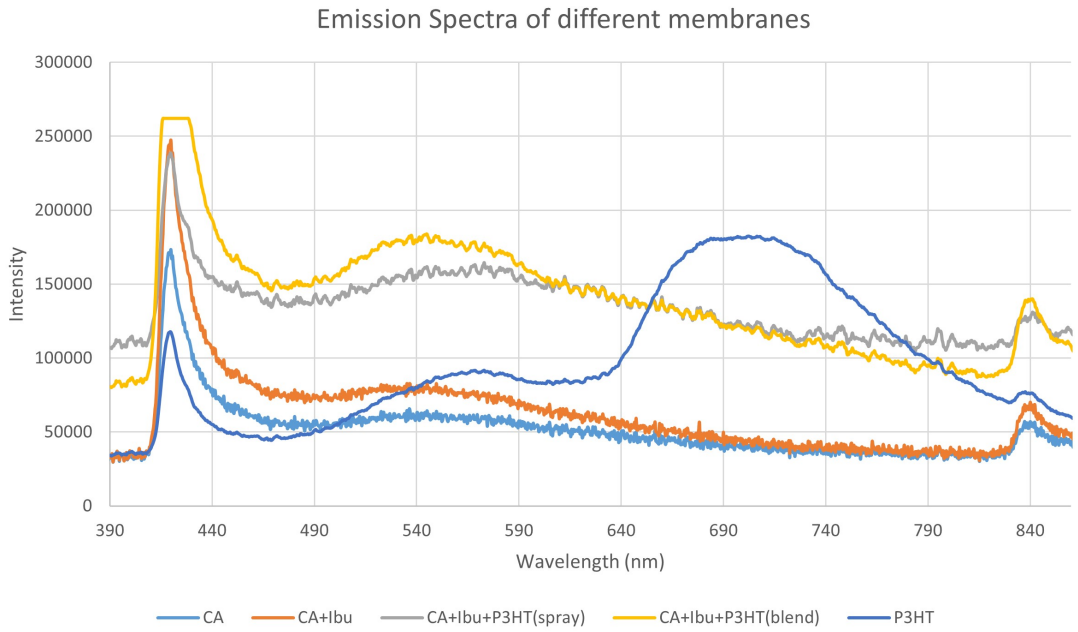


Figure 3.9: Emission spectra of different membranes when excited with a wavelength of 365 nm.

### 3.1.2 Electrical Analysis

An electrical analysis of the different membranes was performed in order to evaluate the effect of the P3HT in the conductivity of the membranes. The membranes were subjected to five different conditions, dark, ambient light, white light, UV and infrared.

To have a level of comparison, a film made of P3HT, without any additives, has an electrical conductivity value of $10^{-4}$ S/cm [35] so, it is expected to see an increase of conductivity in the membranes that have this element in their composition.

The blue marks, representing the CA membrane, consistently exhibit notably low conductivity across all conditions. This outcome aligns with expectations, as the components constituting this membrane lack conductivity capabilities.

By analysis of the graph represented in figure 3.10, the membrane with 8 hours of electrospray, pictured in the graph by the yellow symbols, has the highest conductivity in all the conditions, specifically standing out in the dark and ambient light.

After observing the values obtained for the CA+Ibu+P3HT(spray) membrane that has undergone drug release, purple marks, one can concluded that the process the membrane has undertaken stripped it of its conductive capabilities, especially in conditions where it previously dominated, however it still surpasses the majority of the other membranes, being very close in value with the membrane with 2 hours and 30 minutes of electrospray in every condition except the dark, where the 2 hours and 30 minutes membrane has a higher value.

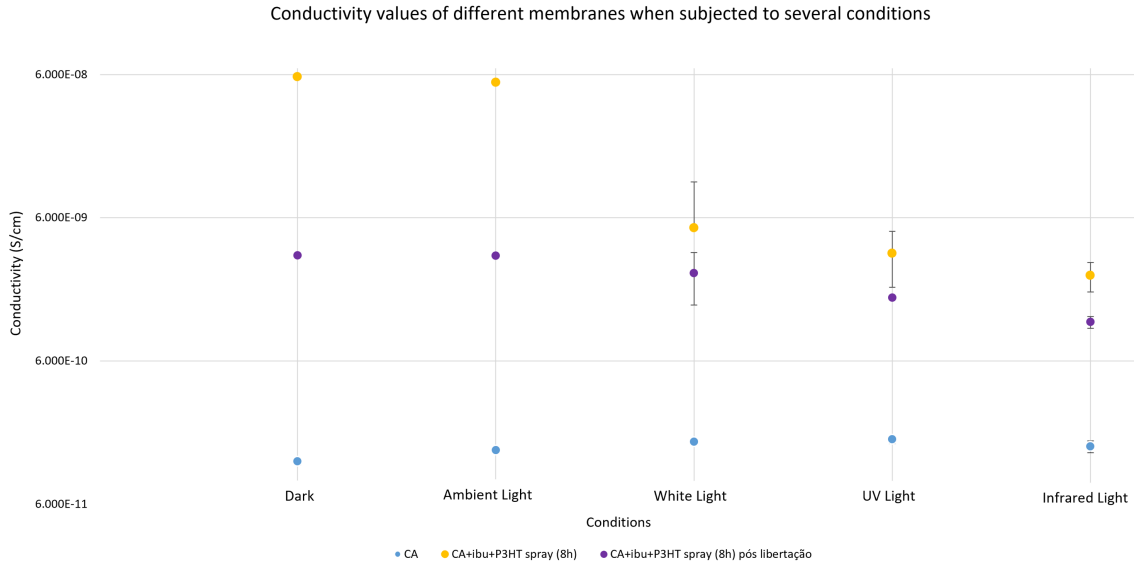


Figure 3.10: Values of conductivity of the membranes in five different conditions.

## 3.2 Drug Release Study

In this section, the calibration curves of Ibu will be presented as well as the results of the various drug release tests made passively and actively.

### 3.2.1 Ibuprofen calibration curve

Given that in the present work two release mediums were used, it was necessary to determine the drug's calibration curve for each of them. The calibration curves were obtained to study the dependence of absorbance on drug concentration, in order to estimate the drug concentration present in the medium during the release assays. Solutions with different concentrations of Ibu were analyzed using UV/visible spectroscopy.

To obtain the calibration curves of Ibu in SBF and in $H_2O$, SBF+Ibu and $H_2O$+Ibu solutions with a concentration of 20 mg/L were prepared, dilutions were made to obtain different concentrations, from 0.5 mg/L to 20 mg/L. The absorbance spectra for both solutions is shown in the figures I.3 and I.4 of annex I.

Absorbance values of each SBF+Ibu concentration were acquired. Following that, for each concentration, the values corresponding to 210 and 222 nm were organized in a absorbance-concentration graph, figure 3.11a, with the linear equations resulting of the mentioned points it is possible to correlate absorbance and concentration. Both equations possess a high correlation coefficient ($R^2$>0.99), however, the 222 nm is more frequently mentioned in literature as a characteristic peak of Ibu [25], for that reason, is the chosen wavelength.

From the chosen SBF+Ibu calibration curve was obtained the following empirical correlation between absorption and Ibu concentration in SBF, equation 3.1.

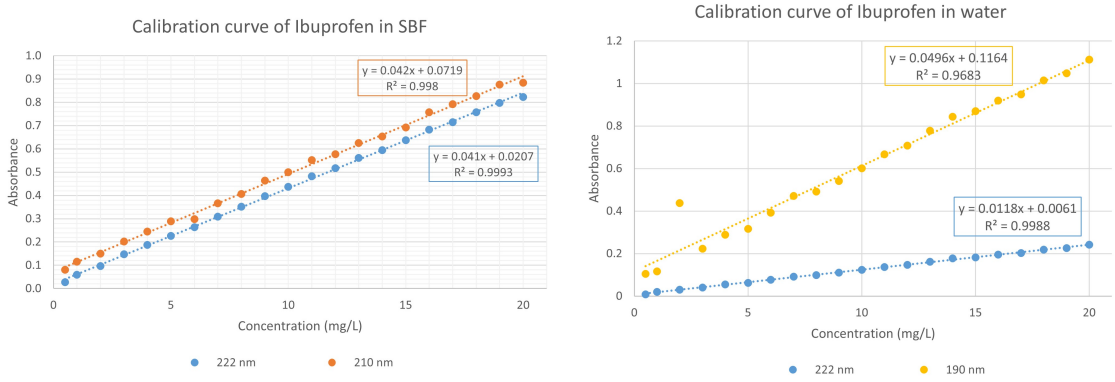


(a) (b)

Figure 3.11: (a) Calibration curves of Ibuprofen in SBF; (b) Calibration curve of Ibuprofen in $H_2O$.

$$[Ibu] = \frac{absorbance - 0.0207}{0.041} \tag{3.1}$$

The same process as previously explained was repeated for the $H_2O$+Ibu concentrations. In this case, the analysed wavelengths were 190 and 222 nm because this were the predominant peaks observed in the absorption spectra. In figure 3.11b are represented the equations and correlation coefficient of each curve, since the correlation coefficient is higher in the 222 nm curve and the 190 nm peak is associated with the absorbance levels of water, the first was the chosen calibration curve, which empirical correlation between absorption and Ibu concentration is represented in equation 3.2.

$$[Ibu] = \frac{absorbance - 0.0061}{0.0118} \tag{3.2}$$

### 3.2.2 Influence of Ultraviolet light on the absorbance of SBF, water and ibuprofen

As a way to verify that the use of SBF wouldn't influence the absorbance results and, consequently, the conclusions on Ibuprofen release from the membranes, this study was conducted.

Table 3.1: Variation of absorbance of $H_2O$, SBF and ibuprofen solutions when exposed to UV light.

| Solution | First Point | Last Point | Variation (%) |
|---|---|---|---|
| $H_2O$ | 0.04 | 0.12 | 8 |
| $H_2O$+Ibu | 2.01 | 2.05 | 4 |
| SBF | 0 | 0.42 | 43 |
| SBF+Ibu | 0.74 | 1.08 | 34 |

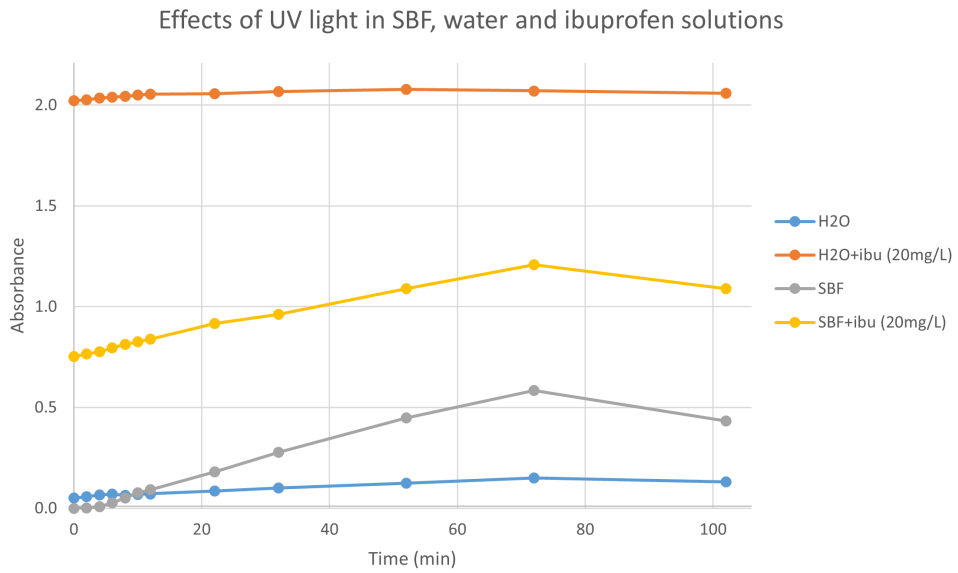


Figure 3.12: Influence of UV light on the absorbance of SBF, water and ibuprofen solutions.

From figure 3.12 and table 3.1 the following conclusions can be drawn, the solutions that contain water have a minor variation when exposed to the UV light, on the contrary, the solutions made with SBF have a significant variation. Comparing the values, the variation of SBF is 35% bigger than the variation of $H_2O$ and the variation of SBF+Ibu is 30% bigger than the variation of $H_2O$+Ibu. Therefore the medium chosen for the drug releases is water as a way of ensuring that the results obtained mainly reflect the influence of Ibuprofen in the medium.

### 3.2.3 Drug release from the membranes

All release assays were conducted following the same procedure to minimize experimental error. In this section, we present the results obtained in the drug release assays passively, through the diffusion process, as well as with the application of stimulus, namely, with the incidence of specific radiation.

#### 3.2.3.1 Passive drug release

In figure 3.13 the passive release, carried out for 9 days, of each of the membranes fabricated is displayed.

Observing the curves, we can conclude that the gray curve, which represents the CA+ibu+P3HT membrane produced by electrospray, exhibits significantly higher values than the other curves. This is due to its thickness, (0.27 ± 0.01) mm, which is twice that of the other membranes, (0.11 ± 0.01) mm, despite being manufactured using the same electrospinning parameters and the same volume of solution. To address this error, the absorbance values of this membrane were divided by two in order to achieve the values of

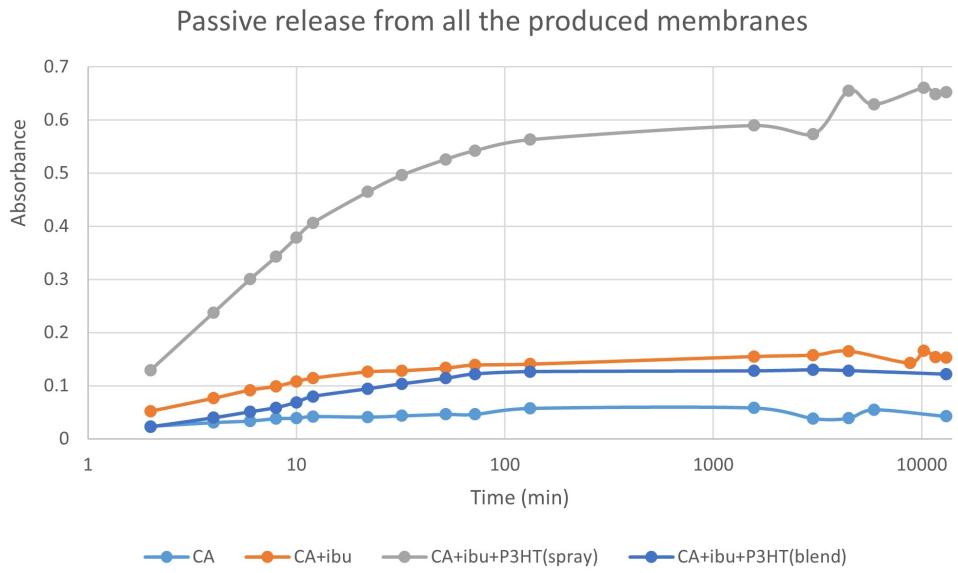


Figure 3.13: Passive release from all the produced membranes.

a membrane with a similar thickness to the other membranes, the yellow curve in figure 3.14 represents that alteration.

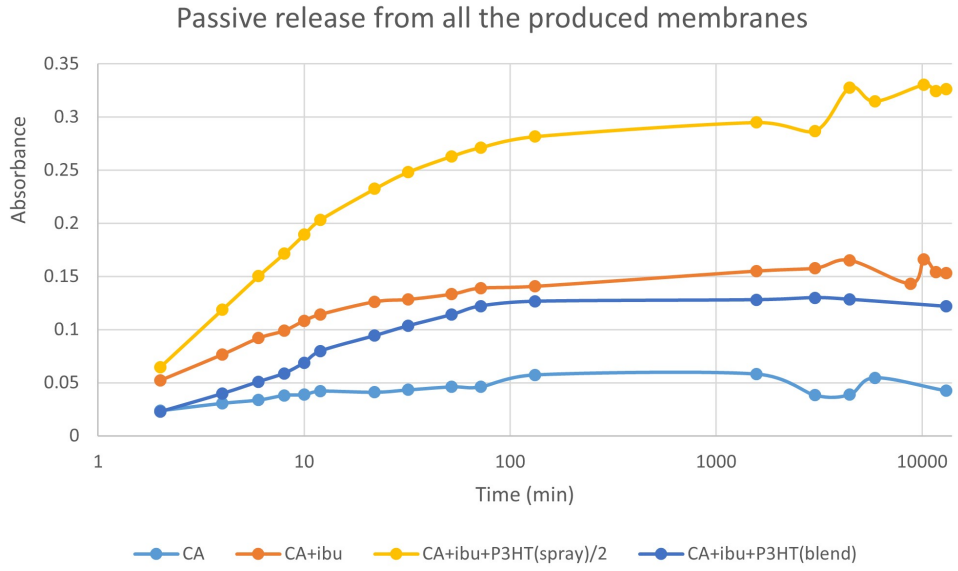


Figure 3.14: Passive release from all the produced membranes with estimated similar thicknesses.

By paying attention to the evolution of the curves in figure 3.14, we can observe that from the 2-hour mark of the study, there is a stabilization of absorbance values in the membranes.

As for the light blue curve, which corresponds to a CA membrane, it should not exhibit such a variation in the absorbance values. However, this is not the case because the

polymer itself can degrade when in contact with water [36].

The CA+Ibu+P3HT(spray) membrane presents much higher values than the other membranes due to it's thickness, however, in the CA+Ibu+P3HT(blend) membrane a lower absorbance value is verified when compared with the CA+Ibu membrane, although a significant variation is not clear, it may be indicative that P3HT may be retaining drug diffusion.

#### 3.2.3.2 Active drug release

In the two active drug releases, which use a UV and an infrared light, we observe the same problem as previously explained, the degradation of the CA membrane. Due to this problem, when exposed to UV light, the membrane reaches much higher absorbance values than in the passive release and, when exposed to infrared light, it reaches higher values than the passive release but lower values than the UV light, this can be observed in figure 3.15.

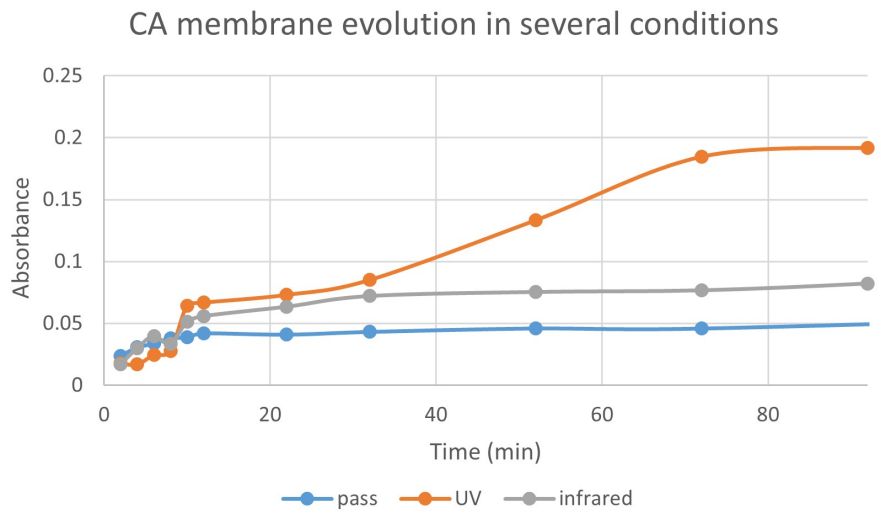


Figure 3.15: CA membrane concentration evolution in passive, UV light and infrared conditions.

Inspecting figure 3.16, where the different membranes subjected to UV light and passive release are compiled, it is visible that the dotted curves, correspondent with the UV light release reach higher levels of Ibu concentration than the full curves, which represent the passive release of the different membranes.

The CA+Ibu and the CA+Ibu+P3HT(blend) membranes start increasing their concentration value, in comparison with the correspondent passive release value, in the early stages of the study whereas the CA+Ibu+P3HT(spray) membrane only overcomes its passive value around the 1 hour mark of the study.

In the case of the membranes exposed to infrared light, present in figure 3.17, this membranes release less Ibu or take more time to reach the same concentration than the

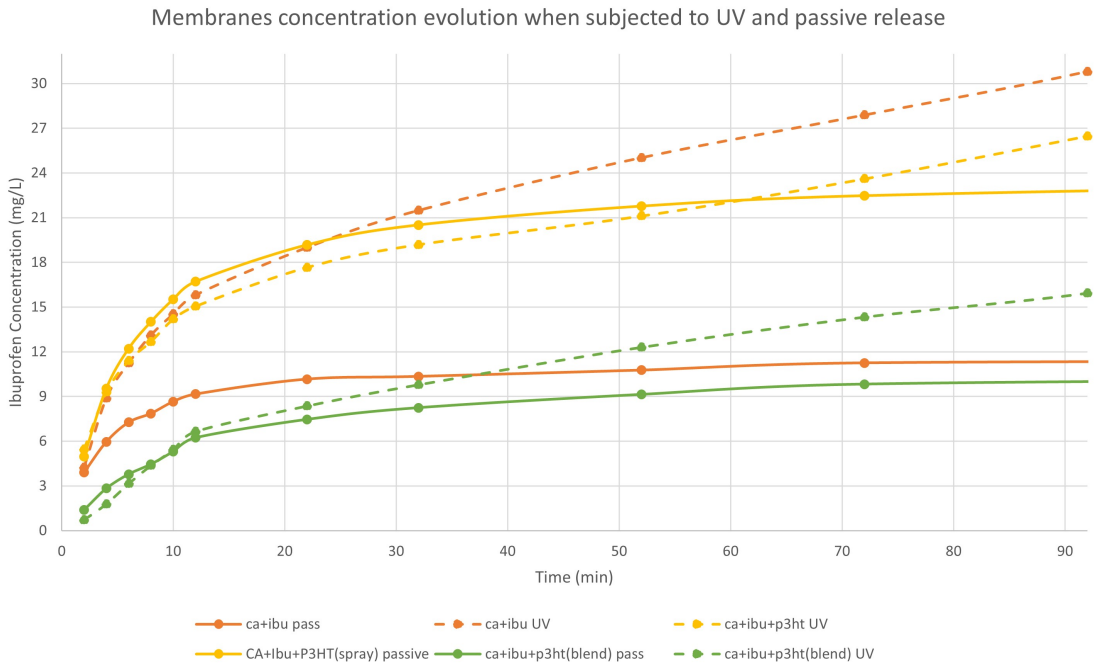


Figure 3.16: Membranes concentration evolution when subjected to UV and passive release.

passive membranes.

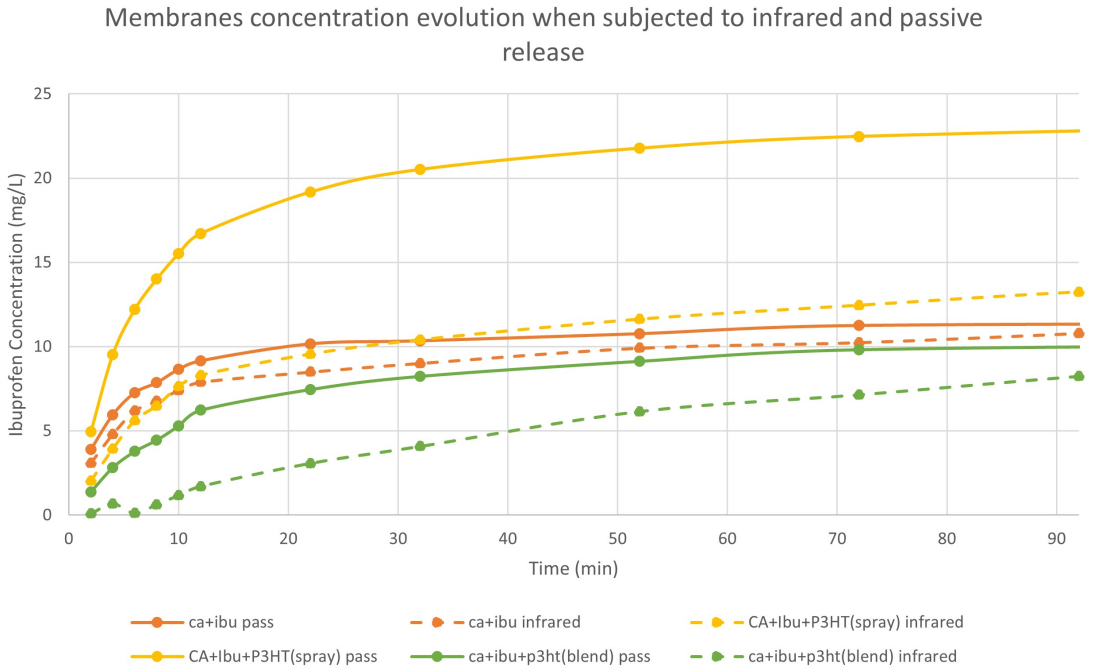


Figure 3.17: Membranes concentration evolution when subjected to infrared and passive release.

The CA+Ibu and the CA+Ibu+P3HT(blend) membranes are very close to reaching the

same value as the passive release at around the 92 minute mark in the study, while the CA+Ibu+P3HT(spray) membrane never reaches its passive concentration value.

In order to objectively analyse the difference between the Ibu concentration values these were compiled into table 3.2.

Table 3.2: Ibuprofen concentration values at the 72 minute mark of the passive, UV and infrared drug releases of the three membranes developed.

| Membranes | Ibu Concentration (mg/L) | | |
|---|---|---|---|
| | Passive | UV | Infrared |
| CA+ibu | 11.25 | 27.89 | 10.24 |
| CA+ibu+P3HT(spray) | 22.47 | 23.60 | 12.45 |
| CA+ibu+P3HT(blend) | 9.83 | 14.33 | 7.14 |

By observation of the different membranes concentration evolution in distinct conditions, we observe that the CA+Ibu membrane has a passive release value of 11.25 g/mol, a higher UV release value at 27.89 g/mol and a lower infrared release value at 10.24 g/mol when compared with the passive. This trend is also verified in the other membranes, the CA+Ibu+P3HT(spray) has a passive value of 22.47 g/mol, an UV value of 23.60 g/mol and an infrared value of 12.45 g/mol, regarding the CA+Ibu+P3HT(blend), the passive value is 9.83 g/mol, the UV is 14.33 g/mol and the infrared 7.14 g/mol. It can be concluded that UV light reaches higher concentration levels than passive release, and infrared light reaches lower concentrations than the previously mentioned conditions.

With this information, the setups with P3HT can be used to, with UV light, increase the drug delivery, and with infrared light, slow down the delivery, working like a switch to ensure the necessary action when needed.

# 4

# Conclusions and future prospects

In this work, different systems for controlled drug release were tested. The drug tested was Ibuprofen, one of the most common anti-inflammatory drugs.

The first constructed system consisted of incorporating the drug into a CA membrane produced by electrospinning and covering said membrane with P3HT by electrospray. The second system was composed by the electrospinning of a solution with the CA, Ibuprofen and P3HT. The drug release of these membranes is controlled by exposure to different lights (UV and infrared) since a photosensitive polymer, P3HT, is incorporated.

The SEM images confirmed the presence of fibers in all the developed membranes with a range of diameters (336 to 1788 nm) where the CA+Ibu+P3HT(blend) membrane had the bigger fibers followed by the CA+Ibu+P3HT(spray) membrane, after being submitted to drug release test all the membranes maintained their integrity and decreased their respective MFD.

The fluorescence spectroscopy and microscopy tests confirmed the presence of P3HT in the CA+Ibu+P3HT(spray) and CA+Ibu+P3HT(blend) membranes having similar values.

In the electrical conductivity test, the CA+Ibu+P3HT(spray) membrane stands out from the others, exhibiting significantly higher values under both dark and ambient light conditions when compared to the other membranes.

The obtained membranes and correspondent drug release results lead to the conclusion that both setups developed are able to control the release of the drug when exposed to different radiations.

In future studies, in order to obtain better statistics, it will be necessary to take into account result verification by conducting a greater number of trials. To improve the performance of the produced membranes, it will be necessary to optimize the amount of incorporated drug and the electrospinning conditions to produce fibers with more uniform thicknesses. Given the available time for this study, it was not possible to optimize the radiation exposure times or the concentration of P3HT contained in the membranes for better control of drug release.

# Bibliography


[1] J. M. Lourenço, *The NOVAthesis LaTeX Template User's Manual*, NOVA University Lisbon, 2021 (cit. on p. ii).

[2] R. F. Rushmer, K. J. K. Buettner, and J. M. Short, "The skin", *New Series*, vol. 154, pp. 343–348, 3747 1966-10 (cit. on p. 1).

[3] V. Falanga *et al.*, "Chronic wounds", *Nature Reviews Disease Primers*, vol. 8, p. 50, 1 2022-07, ISSN: 2056-676X. DOI: 10.1038/s41572-022-00377-3 (cit. on p. 1).

[4] K. Järbrink *et al.*, "The humanistic and economic burden of chronic wounds: A protocol for a systematic review", *Systematic Reviews*, vol. 6, p. 15, 1 2017-12, ISSN: 2046-4053. DOI: 10.1186/s13643-016-0400-8 (cit. on p. 1).

[5] H. S. Kim, X. Sun, J.-H. Lee, H.-W. Kim, X. Fu, and K. W. Leong, "Advanced drug delivery systems and artificial skin grafts for skin wound healing", *Advanced Drug Delivery Reviews*, vol. 146, pp. 209–239, 2019-06, ISSN: 0169409X. DOI: 10.1016/j.addr.2018.12.014 (cit. on p. 1).

[6] Y. Tao, H. F. Chan, B. Shi, M. Li, and K. W. Leong, "Light: A magical tool for controlled drug delivery", *Advanced Functional Materials*, vol. 30, p. 2 005 029, 49 2020-12, ISSN: 1616-301X. DOI: 10.1002/adfm.202005029 (cit. on pp. 1, 4).

[7] J. Rojo, A. Sousa-Herves, and A. Mascaraque, "Perspectives of carbohydrates in drug discovery", in Elsevier, 2017-01, vol. 1-8, pp. 577–610, ISBN: 9780128032008. DOI: 10.1016/B978-0-12-409547-2.12311-X (cit. on p. 2).

[8] J. Zhang *et al.*, "Stimuli-responsive nanoparticles for controlled drug delivery in synergistic cancer immunotherapy", *Advanced Science*, vol. 9, p. 2 103 444, 5 2022-02, ISSN: 2198-3844. DOI: 10.1002/advs.202103444 (cit. on p. 2).

[9] V. W. Karisma *et al.*, "Uva-triggered drug release and photo-protection of skin", *Frontiers in Cell and Developmental Biology*, vol. 9, 2021-02, ISSN: 2296-634X. DOI: 10.3389/fcell.2021.598717 (cit. on pp. 2, 3).

[10] X. Wang, Z. Xuan, X. Zhu, H. Sun, J. Li, and Z. Xie, "Near-infrared photoresponsive drug delivery nanosystems for cancer photo-chemotherapy.", *Journal of nanobiotechnology*, vol. 18, p. 108, 1 2020-08, ISSN: 1477-3155. DOI: 10.1186/s12951-020-00668-5 (cit. on p. 3).

[11] S. K. Rastogi *et al.*, "Enhanced release of molecules upon ultraviolet (uv) light irradiation from photoresponsive hydrogels prepared from bifunctional azobenzene and four-arm poly(ethylene glycol)", *ACS Applied Materials & Interfaces*, vol. 10, pp. 30 071–30 080, 36 2018-09, ISSN: 1944-8244. DOI: 10.1021/acsami.6b16183 (cit. on pp. 4, 35).

[12] M. Ghani *et al.*, "On-demand reversible uv-triggered interpenetrating polymer network-based drug delivery system using the spiropyran-merocyanine hydrophobicity switch", *ACS applied materials & interfaces*, vol. 13, pp. 3591–3604, 3 2021-01, ISSN: 1944-8252. DOI: 10.1021/ACSAMI.0C19081 (cit. on pp. 4, 35).

[13] M. Wang *et al.*, "Gold nanoshell coated thermo-ph dual responsive liposomes for resveratrol delivery and chemo-photothermal synergistic cancer therapy †", *J. Mater. Chem. B*, vol. 5, p. 2161, 2017. DOI: 10.1039/c7tb00258k (cit. on pp. 4, 35).

[14] G. Jin, M. P. Prabhakaran, D. Kai, M. Kotaki, and S. Ramakrishna, "Electrospun photosensitive nanofibers: Potential for photocurrent therapy in skin regeneration", *Photochemical & Photobiological Sciences*, vol. 12, pp. 124–134, 1 2012-01, ISSN: 1474-905X. DOI: 10.1039/c2pp25070e (cit. on pp. 4, 5, 35).

[15] B. Lago, M. Brito, C. M. M. Almeida, I. Ferreira, and A. C. Baptista, "Functionalisation of electrospun cellulose acetate membranes with pedot and ppy for electronic controlled drug release", *Nanomaterials*, vol. 13, p. 1493, 9 2023-04, ISSN: 2079-4991. DOI: 10.3390/nano13091493 (cit. on pp. 4, 16, 35).

[16] M. A. A. Khalek, S. A. A. Gaber, R. A. El-Domany, and M. A. El-Kemary, "Photoactive electrospun cellulose acetate/polyethylene oxide/methylene blue and trilayered cellulose acetate/polyethylene oxide/silk fibroin/ciprofloxacin nanofibers for chronic wound healing", *International Journal of Biological Macromolecules*, vol. 193, pp. 1752–1766, 2021-12, ISSN: 01418130. DOI: 10.1016/j.ijbiomac.2021.11.012 (cit. on pp. 4, 35).

[17] K. Kalwar and M. Shen, "Electrospun cellulose acetate nanofibers and au@agnps for antimicrobial activity - a mini review", *Nanotechnology Reviews*, vol. 8, pp. 246–257, 1 2019-11, ISSN: 2191-9097. DOI: 10.1515/ntrev-2019-0023 (cit. on p. 5).

[18] B. Pant, M. Park, and S.-J. Park, "Drug delivery applications of core-sheath nanofibers prepared by coaxial electrospinning: A review", *Pharmaceutics*, vol. 11, p. 305, 7 2019-07, ISSN: 1999-4923. DOI: 10.3390/pharmaceutics11070305 (cit. on p. 5).

[19] K. Khoshnevisan *et al.*, "Cellulose acetate electrospun nanofibers for drug delivery systems: Applications and recent advances", *Carbohydrate Polymers*, vol. 198, pp. 131–141, 2018-10, ISSN: 01448617. DOI: 10.1016/j.carbpol.2018.06.072 (cit. on p. 5).

[20] G. Jin, M. P. Prabhakaran, S. Liao, and S. Ramakrishna, "Photosensitive materials and potential of photocurrent mediated tissue regeneration", *Journal of Photochemistry and Photobiology B: Biology*, vol. 102, pp. 93–101, 2 2011-02, ISSN: 10111344. DOI: 10.1016/j.jphotobiol.2010.09.010 (cit. on pp. 5, 6).

[21] K. Tremel and S. Ludwigs, "Morphology of p3ht in thin films in relation to optical and electrical properties", in Springer New York LLC, 2014, vol. 265, pp. 39–82. DOI: 10.1007/12_2014_288 (cit. on p. 5).

[22] M. Böckmann, T. Schemme, D. H. D. Jong, C. Denz, A. Heuer, and N. L. Doltsinis, "Structure of p3ht crystals, thin films, and solutions by uv/vis spectral analysis", *Physical Chemistry Chemical Physics*, vol. 17, pp. 28 616–28 625, 43 2015-10, ISSN: 14639076. DOI: 10.1039/C5CP03665H (cit. on p. 5).

[23] R. Bushra and N. Aslam, "An overview of clinical pharmacology of ibuprofen", *Oman Medical Journal*, vol. 25, pp. 155–161, 3 2010-07, ISSN: 1999768X. DOI: 10.5001/omj.2010.49 (cit. on p. 6).

[24] M. Abualhasan, M. Assali, A. n. Zaid, R. Tarayra, A. Hamdan, and R. Ardah, "Synthesis and formulation of ibuprofen pro-drugs for enhanced transdermal absorption", *international journal of pharmacy and pharmaceutical sciences*, vol. 7, pp. 352–354, 2015-02 (cit. on p. 6).

[25] A. Tewari, A. Bagchi, A. Raha, P. Mukherjee, and M. Pal, "Preparation, estimation and validation of the parameters of the standard curve of ibuprofen by comparative study", *Asian Journal of Pharmacy and Pharmacology*, vol. 3, pp. 79–85, 3 2017-07 (cit. on pp. 6, 23).

[26] A. Celebioglu and T. Uyar, "Electrospun porous cellulose acetate fibers from volatile solvent mixture", *Materials Letters*, vol. 65, pp. 2291–2294, 14 2011-07, ISSN: 0167577X. DOI: 10.1016/j.matlet.2011.04.039 (cit. on pp. 8, 18, 19).

[27] M. Roesing, J. Howell, and D. Boucher, "Solubility characteristics of poly(3-hexylthiophene)", *Journal of Polymer Science Part B: Polymer Physics*, vol. 55, pp. 1075–1087, 14 2017-07, ISSN: 08876266. DOI: 10.1002/polb.24364 (cit. on p. 8).

[28] M. Wang and Q. Zhao, "Electrospinning and electrospray for biomedical applications", in Elsevier, 2019-01, vol. 1-3, pp. 330–344, ISBN: 9780128051443. DOI: 10.1016/B978-0-12-801238-3.11028-1 (cit. on pp. 9, 16, 17).

[29] J. Sanderson, "Fundamentals of microscopy", *Current Protocols in Mouse Biology*, vol. 10, 2 2020-06, ISSN: 2161-2617. DOI: 10.1002/cpmo.76 (cit. on p. 10).

[30] M. J. Sanderson, I. Smith, I. Parker, and M. D. Bootman, "Fluorescence microscopy", *Cold Spring Harbor Protocols*, vol. 2014, pdb.top071795, 10 2014-10, ISSN: 1940-3402. DOI: 10.1101/pdb.top071795 (cit. on p. 10).

[31] J. Lodge, *Methods of Air Sampling and Analysis*, J. P. Lodge, Ed. Routledge, 2017-11, pp. 187–190, ISBN: 9780203747407. DOI: 10.1201/9780203747407 (cit. on p. 11).

[32] T. Kokubo and H. Takadama, "How useful is sbf in predicting in vivo bone bioactivity?", *Biomaterials*, vol. 27, no. 15, pp. 2907–2915, 2006, ISSN: 0142-9612. DOI: https://doi.org/10.1016/j.biomaterials.2006.01.017 (cit. on p. 12).

[33] S. Görög, *Ultraviolet-Visible Spectrophotometry in Pharmaceutical Analysis*. CRC Press, 2018-01, pp. 1–391, ISBN: 9781351077422. DOI: 10.1201/9781351077422 (cit. on p. 12).

[34] X.-T. Hao, L. M. Hirvonen, and T. A. Smith, "Nanomorphology of polythiophene–fullerene bulk-heterojunction films investigated by structured illumination optical imaging and time-resolved confocal microscopy", *Methods and Applications in Fluorescence*, vol. 1, p. 015 004, 1 2013-01, ISSN: 2050-6120. DOI: 10.1088/2050-6120/1/1/015004 (cit. on p. 20).

[35] E. Lim, K. A. Peterson, G. M. Su, and M. L. Chabinyc, "Thermoelectric properties of poly(3-hexylthiophene) (p3ht) doped with 2,3,5,6-tetrafluoro-7,7,8,8-tetracyanoquinodimethane (f <sub>4</sub> tcnq) by vapor-phase infiltration", *Chemistry of Materials*, vol. 30, pp. 998–1010, 3 2018-02, ISSN: 0897-4756. DOI: 10.1021/acs.chemmater.7b04849 (cit. on p. 22).

[36] C. R. Nascimento, "Estimulação com radiação para controlo da libertação de fármaco em filmes para aplicações dérmicas", 2023-03 (cit. on p. 27).

# I

# Annex 1

## I.1 State of the Art

Table I.1: Stimuli controlled DDSs.

| System | Stimulus | Materials | Applications | Ref. |
|---|---|---|---|---|
| Hydrogel | UV/photoisomerization | Azobenzene, PEG | Drug release | [11] |
| | UV/photoisomerization, induced volumetric change | Silicone, Spiropyran and merocyanine | In vitro doxorubicin release | [12] |
| Nanomaterials | pH and NIR | Gold nanoshell-coated chitosan liposomes | Resveratrol drug delivery | [13] |
| Fibers | Visible light | PCL and P3HT | Tissue regeneration | [14] |
| | Electric potencial | CA, Poly(3,4-ethylenedioxy thiophene) and Ibu | Controlled drug release | [15] |
| | Red light | CA, polyethylene oxide and methylene blue | Preventing the development of bacteria | [16] |

## I.2 Current-Voltage Characteristic Curve

In figure I.1 is a typical Current-Voltage Curve. According to Ohm's Law,

$$V = R \times I \tag{I.1}$$

where the current passing through the device is a function of the applied potential, as $I$ is proportional to the potential difference, $V$, multiplied by the proportionality constant, $\frac{1}{R}$.

Therefore, in an ideal resistance, this relationship is linear, making $\frac{1}{R}$ the slope of the line representing the current against the potential difference. Hence, by obtaining the I-V curves and calculating the resistance ($R$), the conductivity of the membrane is determined by the following expression,

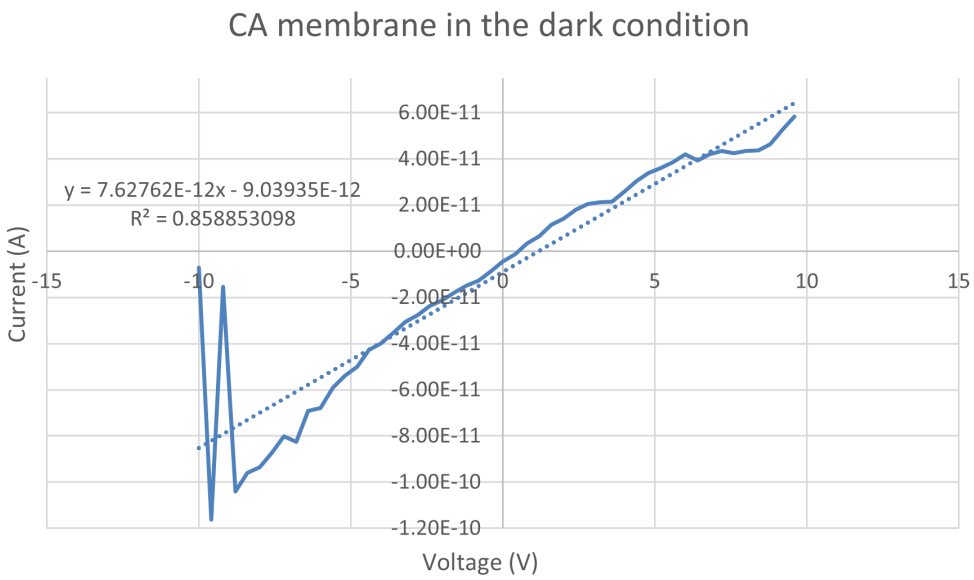


Figure I.1: I-V Curve of CA membrane when exposed to the dark.

$$\sigma = \frac{l}{A \times R} \tag{I.2}$$

Where $\sigma$ represents the electrical conductivity ($S/cm$), $R$ is the resistance ($\Omega$) obtained from the slope of the I-V line, $A$ is the cross-sectional area of the membrane through which the current passes ($cm^2$), and $l$ is the distance between the electrodes ($cm$).

In figure I.2 is represented a diagram of a membrane with the two electrodes, made with carbon conducting ink, which measure 5 mm in length, which multiplied by the thickness of the membrane makes up the cross-sectional area, $A$, and a distance between electrodes, $l$, of 2 mm.

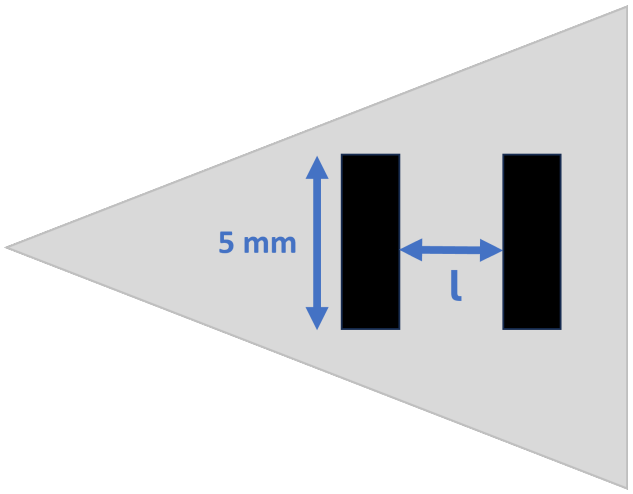


Figure I.2: Diagram of the membrane setup utilized for the I-V Curve.

## I.3 Ibuprofen calibration curve

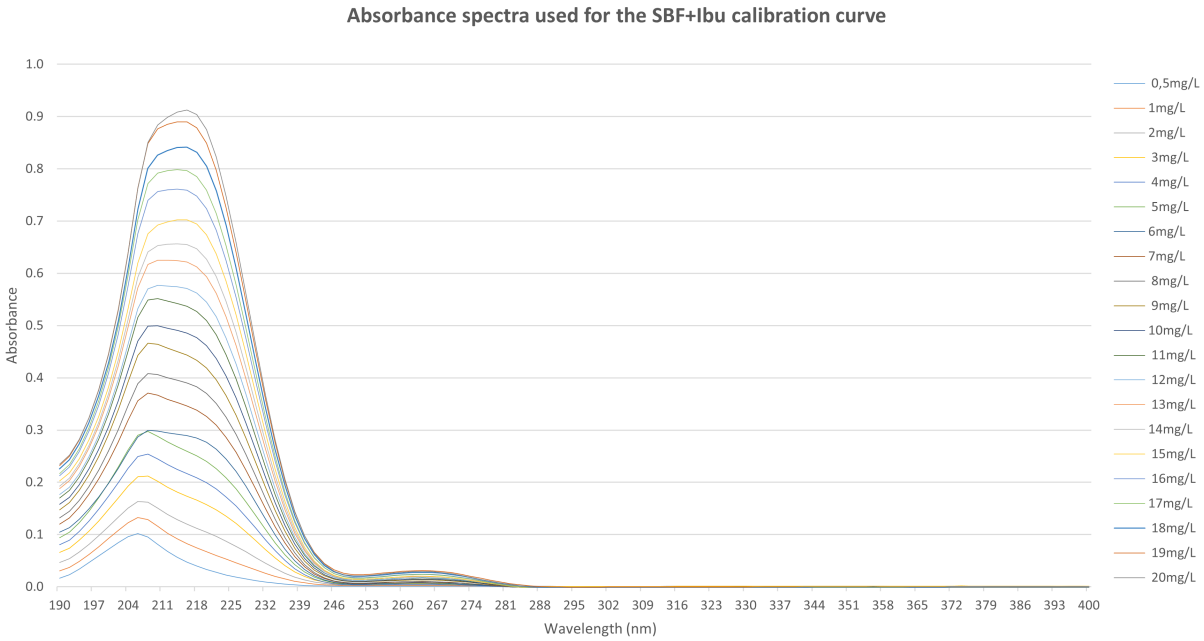


Figure I.3: Absorbance spectra used for the SBF+Ibu calibration curve.

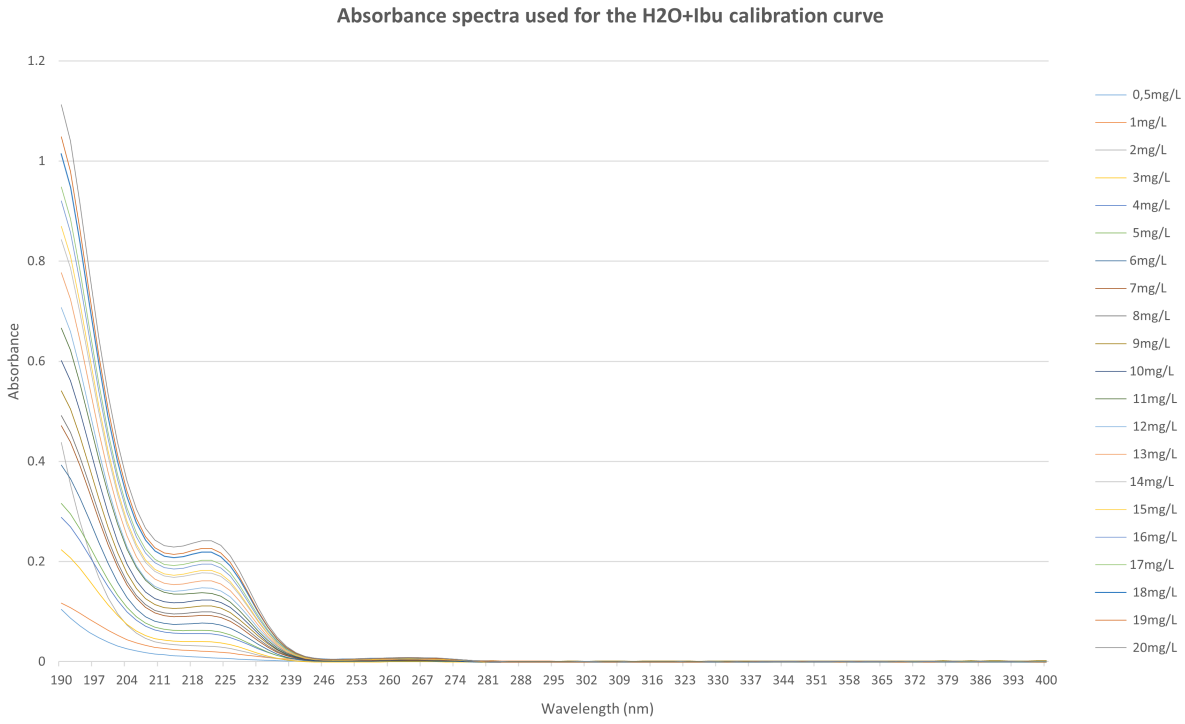


Figure I.4: Absorbance spectra used for the $H_2O$+Ibu calibration curve.